In Vitro Assessment of Bone and Cartilage Stimulating Peptides

by

Bowen Yang

A thesis submitted to the Department of Chemical Engineering

in conformity with the requirements for

the degree of Master of Applied Science

Queen's University

Kingston, Ontario, Canada

April, 2016

Abstract

Spinal fusion is an effective and one of the most commonly used surgeries to treat intervertebral disc degeneration (IDD) related low back pain. However, non-fusion still occurs in about 10-15% of the clinical cases. The global objective of this project is to develop a synthetic bone graft for the spinal fusion, combined with bone growth enhancing factors named bone and cartilage stimulating peptides (BCSP®). The focus of this present study is to assess BCSPs' performance in various concentrations with respect to their effects on osteoprogenitor proliferation, osteogenic differentiation, cell culture mineralization and cell migration.

BCSPs appeared to enhance the bone growth in the previous study using an animal model; however, the cellular and molecular mechanisms of BCSPs performance remain unclear. In this study, we examined three BCSPs *in vitro* with respect to their ability to enhance proliferation, to induce early osteogenic differentiation and mineralization, and to simulate the migration of osteoprogenitor cells. The proliferation, early differentiation, mineralization and migration assessments were carried out with a double-stranded DNA quantification, an alkaline phosphatase (ALP, early osteogenic differentiation marker) expression assay, an Alizarin Red S staining assay and a Boyden Chamber assay, respectively. Osteoprogenitor cells examined included MC3T3-E1 preosteoblasts, human bone marrow-derived mesenchymal stem cells (hBM-MSCs), human periosteum-derived stem cells (hPDSCs), and rabbit periosteum-derived stem cells (rPDSCs).

Both hBM-MSCs and MC3T3-E1 preosteoblasts exhibited a significant increase of ALP expression after the exposure to BCSP1 and BCSP7, and MC3T3-E1 preosteoblasts also exhibited a significant increase of ALP expression after the exposure to BCSP11. However, no significant difference was observed in proliferation, migration or mineralization assessments for any of the examined osteoprogenitor cells after exposure to BCSPs. The present work showed that BCSPs have a stimulating effect on the early differentiation of MC3T3-E1 preosoteblast and human BM-MSCs. However, BCSPs did not show any stimulating effects on the proliferation, mineralization and migration of osteoprogenitors listed, indicating that promoting early differentiation of osteoprogenitors might be one of the mechanisms of BCSPs' *in vivo* bone growth stimulating effect.

Acknowledgments

I would like to express my sincere gratitude to my supervisor Dr. Brian Amsden for his guidance, support and patience. This opportunity that he gives me to come to Queen's University and work for him as his student is absolutely life-changing and I will always be grateful for that.

I would like to thank our lab manager Dr. Dale Marecak for his support and help during my studies. I would also like to thank Dr. Roshni Rainbow, Dr. Gad Sabbatier, Andrew Carroll, Claire Yu, Dr. Valerio Russo, Stuart Young, Lydia Fütterer, Bryen Turco, Tim Han, Dr. Fei Chen, Dimitra Louka, William Chaplin, Fiona Serack, Amanda Brissenden, Dr. Moira Vynerfor, Sara Mohajeri, Shadi Taghavi, Julian Chesterman and Ming Gong for taking time to teach me techniques, help me with my experiments and classes or simply have a chat about life. Special thanks to August Xinhai Guo, Jerry Liu, Richard Zhang for being great friends and always supportive.

I would like to take this special chance to thank my mom Linzhi Yang for her unconditional love to me and belief in me, and my dad Jingdong Yu for the motivation, support and guidance he has been providing over the years.

Common Abbreviations

AF	Annulus fibrosus
ALP	Alkaline phosphatase
BCSP	Bone and cartilage stimulating peptide
BMP	Bone morphogenetic protein
BSA	Bovine serum albumin
BSP	Bone sialoprotein
DAPI	4’,6-diamidino-2-phenylindole
DMSO	Dimethyl sulfoxide
dsDNA	Double-stranded DNA
ECM	Extracellular matrix
EDTA	Ethylenediaminetetraacetic acid
FBS	Fetal bovine serum
hBM-MSCs	Human bone marrow-derived mesenchymal stem cells
HLA-DR	Human leukocyte antigen-D related
hPDSCs	Human periosteum-derived stem cells
IDD	Intervertebral disc degeneration
IL-1	Interleukin-1
IL-6	Interleukin-6
MMP	Matrix metalloproteinase
NP	Nucleus pulposus
OC	Osteocalcin
PBS	Phosphate-buffered saline
PDGF	Platelet-derived growth factor
pNP	P-nitrophenyl
rh-FGF-b	Recombinant human basic fibroblast growth factor
rh-IGF-1	Recombinant human insulin-like growth factor 1
rPDSCs	Rabbit periosteum-derived stem cells
Runx2	Runt-related transcription factor 2
TGF-beta	Transforming growth factor beta
TNF-alphaa	Tumor necrosis factor alpha
Tris-Cl	Tris(hydroxymethyl)aminomethane hydrochloride

List of Figures and Tables

Table of Contents

Chapter 1: Introduction

1.1 Clinical Motivation

Worldwide, approximately 80% of the population is affected by low back disease, which gives rise to severely debilitating symptoms (1). Low back pain has become one of the leading causes of function loss with consequent impairment to quality of life, while also contributing to lower work productivity (2). In 1998 in the United States, people suffering from back pain spent $90.7 billion for their healthcare expenses, and what is more alarming is that, healthcare of back pain patients costs 60% more than that of individuals without back pain ($3,498 vs. $2,178) (3). Limited daily activity and reduced capability of working impose a heavy social and economic burden on both individuals and governments (4-6). Intervertebral disc degeneration (IDD) is the leading cause of lower back pain and accounts for 80% to 90% of clinical cases, while neurogenic conditions (e.g., spinal stenosis) and non-mechanical conditions (e.g., infection, inflammation) are the leading causes for the remaining 10-20% of the population with low back pain (7).

In the majority of clinical cases, low back pain is associated with IDD. Magnetic resonance imaging has a long history of being the gold standard for assessing IDD, indicating the strong association between IDD and lower back issues. In addition, a recent study also shows that the correlation between IDD and low back pain symptoms becomes stronger when the global severity of IDD progresses (8). Moreover, the global severity of disc degeneration can also be used to predict the occurrence of first-time low back pain episodes (9). Compared to other musculoskeletal diseases, the occurrence of IDD appears

early, with approximately 20% of the people developing mild disc degeneration in their teenage years. Based on a study with approximately 600 specimens, the incidence of disc degeneration increased sharply with age and exhibited a higher severity in males than females. In the specimens examined, 17% of those who were in their 50s had severe disc degeneration while the percentage increased to 55 of hose who were in their 70s (10).

1.2 Intervertebral Disc

The intervertebral disc is sandwiched between vertebral bodies, and it consists of two parts: the annulus fibrosus (AF), a tough outer fibrous ring, and the nucleus pulpous (NP), an amorphous gelatinous central region [Figure 1]. Cells in the AF have elongated nuclei and align with collagen fibrils, showing a fibroblast-like morphology. Cells in the inner region of the AF show a rounded chondrocyte-like morphology, similar to the cells in the NP. Type II collagen and proteoglycan are produced in the inner region of the AF with type I collagen being the dominant component of the extracellular matrix (ECM) of the AF.

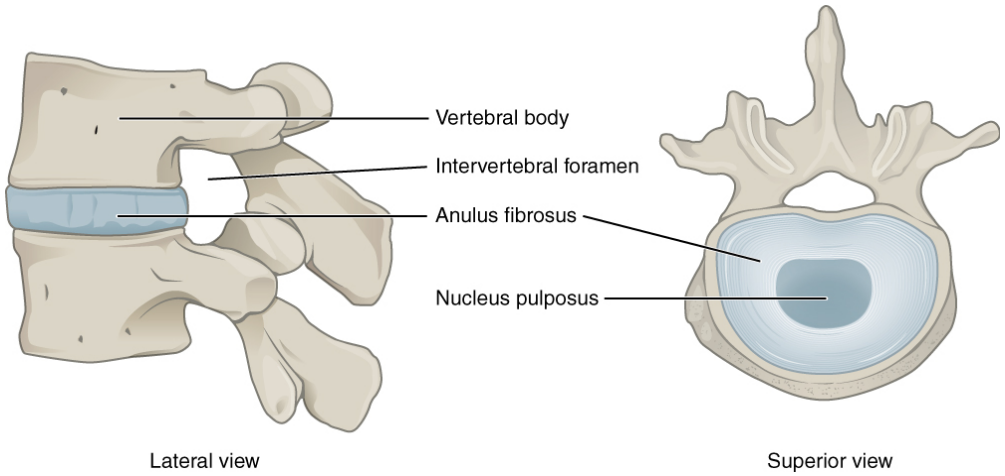

Figure 1. Diagram of intervertebral disk.
Photo credit: OpenStax College, Anatomy & Physiology, Connexions Web site. http://cnx.org/content/col11496/1.6/, Jun 19, 2013. Open access.

Alternatively, the NP has a higher proteoglycan concentration compared to the AF with type II collagen being the dominant type of collagen in the ECM of the NP. In the outer region of the AF, type I collagen represents about 80% of the total collagen. This percentage drops and type II collagen concentration increases towards the central region of the disc. At the AF-NP transition zone, type II collagen accounts for about 80% of the total collagen and type I collagen becomes almost absent (11, 12). Collagen represents approximately 70% of the dry weight of AF and 20% of NP (13).

Intervertebral discs serve as the main joints within the spinal column and take up one-third of the total length. Aggrecan is the major proteoglycan in the intervertebral disc, accounting for approximately 25% of the dry weight of the AF and 70% of the dry weight of the NP (14, 15). Aggrecan is negatively charged due to its disaccharide side chain structure. This negative charge produces an osmotic pressure which acts to maintain disc tissue hydration. With sufficient hydration, the disc possesses a swelling pressure and the latter contributes to compression resistance (16). The sum of the supports from both the AF and the NP is reflected by the disc height, which is maintained and balanced by the tensile strength of the AF and the swelling pressure of the NP (17).

1.3 Function Loss

As described above, the load-bearing property of the intervertebral disc can mainly be attributed to the swelling pressure produced by proteoglycans within the hydrated tissue. Therefore, the loss or reduction of proteoglycans within the extracellular matrix has a markedly negative effect on the intervertebral disc's mechanical function and compression

or load bearing resistance (18). Following the loss of proteoglycan within the disc, resulting in a reduction of osmotic pressure, the disc loses its ability to maintain optimum tissue hydration. Previous research has shown that degenerated discs have a lower water content compared to healthy discs (18), which results in these discs losing height (19) with a concomitant increased risk of bulging of the disc or spinal disc herniation. Major changes of the disc not only affect its function and the adjacent vertebral bodies, but also have a critical influence on the entire spinal structure. The lack of tissue hydration and disc herniation can alter the distribution of loading pressure on the spine (e.g., abnormal pressure may be applied to apophyseal joints) potentially leading to an osteoarthritic condition (20). Work-related injury is one of the leading causes of disc degeneration and structural damage due to the abnormal load distribution (21). Studies using animal models have also indicated that the disc degeneration can be initiated by overload or injury (22, 23).

In addition to the mechanical function changes, loss of proteoglycan also affects the cellular and molecular environment of the disc. When the tissue is healthy, large molecules cannot enter the disc matrix due to the negative charge and the complex structure of aggrecan. Following the loss of proteoglycan, large molecules such as cytokines or growth factors can enter the disc, thereby changing cellular behaviour and the internal environment, which then can accelerate the progression of disc degeneration (21, 24).

1.4 Spinal Fusion

Spinal fusion is one of the most commonly used methods to treat IDD and ease lower back pain symptoms and discomfort. In spinal fusion surgery, two vertebrae are

merged into one, thus eradicating a mobile joint. The degenerated disc between these vertebrae is removed and the two vertebrae are bridged through the ingrowth of the newly formed bone tissue under the guidance of the grafts (25, 26) [Figure 2]. From 2005 to 2008, there were, on average, 360,000 spinal fusion surgeries performed annually in the United States (27). In 2011, the number of spinal fusion procedures increased from 2005-2008 levels to approximately 480,000 and comprised 3.1% of the total number of operating room procedures (28). The number of spinal fusions increased 1.7-fold through 2001 (287,600 cases) to 2011 (29). In the United States, overall spending for spinal fusion surgery in 1998 was estimated to be $4.3 billion, and this had increased to $33.9 billion by 2008, an increase of 7.9 fold, indicating a significant business market for spinal fusion techniques.(27)

However, despite the great number of spinal fusion procedures performed and the improvement in clinical techniques, spinal fusion failure is still a significant occurrence. It has been reported that in 10-15% of clinical cases (30-33), vertebrae and bone grafts do not

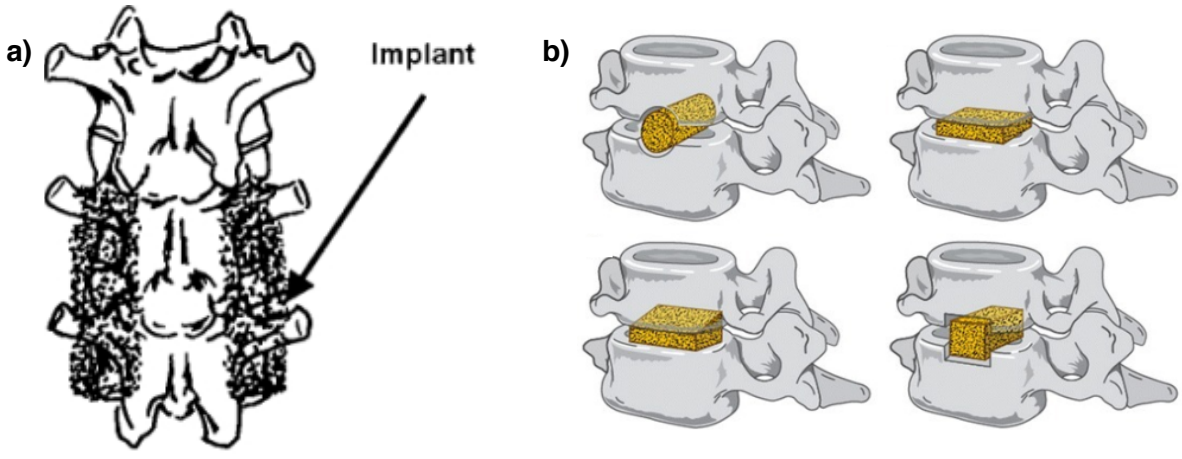

Figure 2. Diagram of spinal fusion techniques. a) Posterolateral fusion, bone grafts were implanted beside the vertebrae and form the bone bridge between transverse processes (25, open access). b) Interbody fusion, bone grafts were placed between vertebrae (26, open access).

fuse thus resulting in a non-union condition where the patient's body sees vertebrae as separated bones and does not guide them to fuse. Poor outcomes in spinal fusion may cause prolonged discomfort to patients and extra procedures to be performed, resulting in a financial burden to patients and stressing the healthcare system. Since 1911, when Hibbs (34) first reported the use of bone tissue harvested from other regions of the patient's body such as the hips, to bind two vertebrae into one, autograft (using bones from the patients themselves) has become the gold standard. However, limited accessibility and serious complications following autograft harvest and spinal fusion surgery (35) are compelling researchers to search for improvements in bone fusion and healing strategies, with advanced scaffolds and bone growth enhancing factors.

1.5 Project Overview

The global objective of this project was to develop a synthetic replacement for bone autograft, consisting of a non-degradable structural polymer and a porous inorganic material, combined with bone growth enhancing factors named bone and cartilage stimulating peptides, or BCSPs. The objective of this present study was to seek an optimal concentration of BCSP for the following drug delivery system design. The improvement of cell proliferation, cell osteogenic differentiation, cell culture mineralization and cell migration were used as parameters to assess various types of BCSP in various concentrations *in vitro*.

Chapter 2: Literature Review

The healing process after the spinal fusion surgery is very similar to the healing process of a critical bone fracture, which includes bone growth and bone remodeling. In this chapter, the fundamental knowledge of bone structure, cell biology of bone tissue, bone remodeling and fracture healing process are introduced, as well as the previous studies involving the activity of the various BCSPs. The objective of this present study and the approaches of experiments are also included in this chapter.

2.1 Bone Anatomy

Bone is a dense connective tissue that protects organs and supports the human body structure. Bone is also the primary reservoir of essential minerals such as calcium, phosphate, magnesium, sodium and carbonate. Erythrocytes, thrombocytes and most of the leukocytes arise from bone marrow (36). Muscles attach to the bone, via tendons, and provide mobility for the human body. Bones are categorized into five types according to the shape: long bones (e.g., femur), short bones (e.g., carpal), flat bones (e.g., frontal) and sesamoid bones (e.g., patella) and irregular bones (e.g., vertebra). Irregular bones have a relatively thin cortical bone layer and a cancellous bone interior (37).

Cortical bones are also known as compact bones, which refer to the hard compact outer layer of bones. Cortical bone consists of highly packed osteon, which is the primary functional unit also referred to as the Haversian system (38). Each osteon has a concentric ring structure termed a lamellae, which is generated by multiple layers of osteoblasts and

osteocytes (trapped and differentiated osteoblasts) and a central tunnel called the Haversian canal. The space where osteoblasts and osteocytes reside is referred to as the lacunae. The network of linked lacunae and Haversian canals is connected by small transverse channels, termed canaliculi, and this network is responsible for the transportation of nutrients to the osteon and the removal of waste products from within the osteon (38). Blood vessels taking up space within the Haversian canals are aligned with the axial direction of osteon cylinders. In contrast, a Volkmann's canal is a perforating canal system that is connected with the Haversian canals, and also consists of blood vessels. Blood vessels in both Volkmann's canals and Haversian canals form a network for the transportation of nutrition from the surface of the bone to the interior. The periosteum covers the outer surface of cortical bones while the endosteum covers the inside surface (37) [Figure 3].

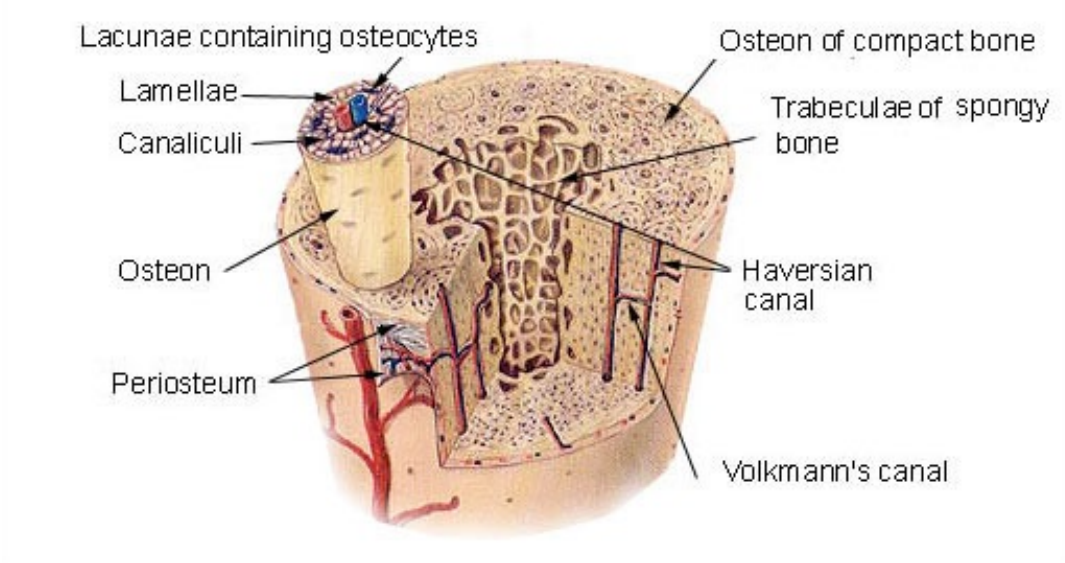

Figure 3. Microscopic diagram of bone structure. (U.S. National Cancer Institute's Surveillance, Epidemiology and End Results (SEER) Program, http://training.seer.cancer.gov/index.html, open access)

Cancellous bone, also known as spongy bone or trabecular bone, makes up around 20% of the total bone mass within the human body. Thin lamellae called trabeculae form a sponge-like porous architecture in cancellous bones in response to the loading and are able to provide an enormously large surface area, as compared to cortical bone, for bone growth and remodeling (39, 40). Cancellous bone also provides space for bone marrow which contains bone-marrow stem cells and produces red blood cells. As the bone matures with age, red bone marrow is replaced by fatty marrow. However in femurs, ribs and the vertebrae of adults, red bone marrow can still be found (41).

2.2 Cell Biology of Bone

2.2.1 Bone Formation, Resorption and Maintenance

Osteoblasts, osteoclasts and osteocytes are essential cells among the cell population in the mature bone tissue and play critical roles in the formation, resorption and maintenance of bone, respectively.

The population of osteoblasts is made up of cells of three differentiation phases: pre-osteoblasts, mature osteoblasts and osteocytes. Both endosteum and periosteum are reservoirs of pre-osteoblast cells (42). Endosteum pre-osteoblasts give rise to mature osteoblasts that are active on the endocortical bone surfaces and trabecular bone surfaces, and which play an important role in maintaining the mechanical function of the skeletal structure. Mature osteoblasts differentiated from periosteum pre-osteoblasts are active on the outer surface of cortical bones. After maturation, osteoblasts are responsible for producing a

matrix known as osteoid. Collagenous proteins, of which 97% are type I collagen and 3% are type V collagen, comprise around 95% of the osteoid secreted by mature osteoblasts. The remaining 5% of the osteoid consists of proteoglycans, water, and non-collagenous proteins, such as osteonectin and sialoproteins (43). Mineralization of the osteoid occurs during the bone remodeling. Prior to mineralization, the osteoid consists largely of organic component and a portion of this is replaced with inorganic compounds as the process of calcification occurs. The mature bone tissue consists of approximately 5% water, approximately 25% organic component that is similar to osteoid (around 90% type I collagen), and the remaining 70% is composed of inorganic calcium and hydroxyapatite (44). Osteoblasts are involved in the mineralization process and release alkaline phosphatase, an enzyme that cleaves the phosphate groups which become the mineral deposition foci (45).

Osteoblasts will undergo either apoptosis, commonly known as programmed cell death, or they will be trapped by the matrix they secreted and eventually differentiate into osteocytes. Osteocytes are the most abundant cells within bone tissue and they play critical roles in bone maintenance, regulation and mineral homeostasis (46). Osteocytes form a communication network with their characteristic elongated plasma membrane and dendritic extensions. One important role of this network is to serve as a mechano-sensing system to regulate bone formation activities and resorption activities of osteoblasts and osteoclasts (47, 48).

Osteoclasts typically reside on the inner surface of the bone, and the bone resorption cavities are known as the Howship's lacunae. They are derived from the fusion of

multiple mononuclear hemopoietic precursors into one multinucleate cell (44). Osteoclasts are responsible for bone resorption by producing hydrolytic enzymes and protons to digest and dissolve the organic and inorganic components of the bone tissue, respectively. Osteoclasts contact bone surfaces with what is called a ruffled border [Figure 4], which provides a large interaction area for resorption (49). The ruffled border attaches to the bone surface and creates a space between the cell and the bone surface, known as the extracellular resorbing compartment. Hydrolytic enzymes, such as the matrix metalloproteases (MMPs) and cathepsin, are produced intracellularly, transported by secondary lysosomes or vesicles, and released into the resorbing compartment (50). H^+-ATPase proton pumps along the

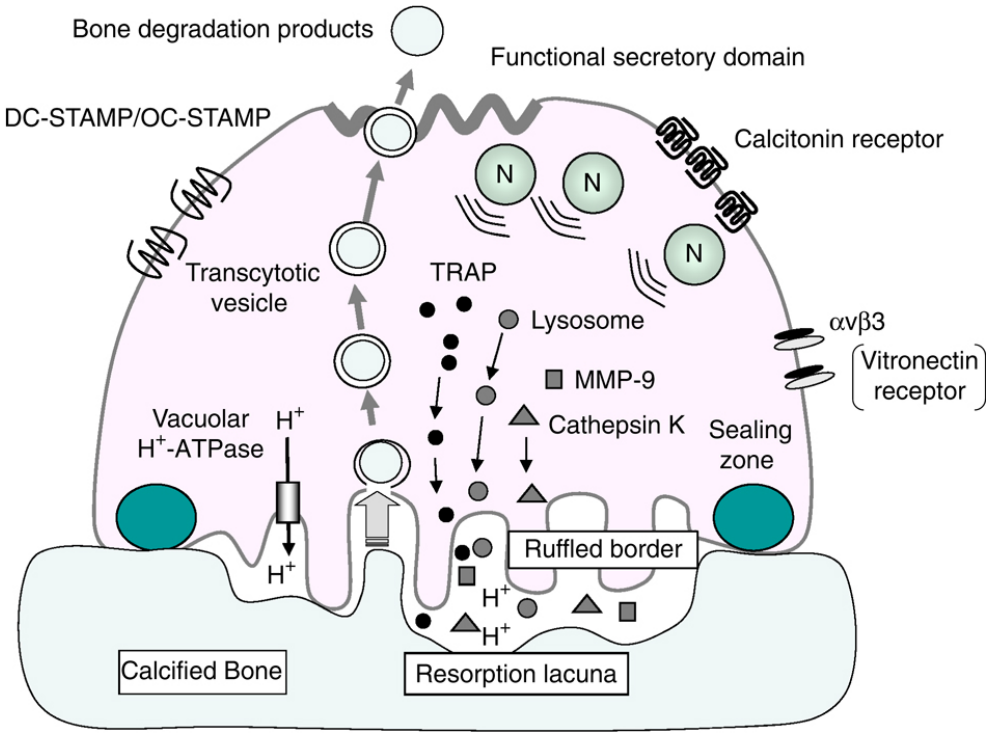

Figure 4. Diagram of osteoclast and ruffled border. (49, used with permission)

ruffled border transport protons from inside the cells, across the cellular membrane into the resorption cavities (51, 52). These protons provide an ideal pH to promote and stimulate the hydrolytic process (51, 53). As a result of the secretion of protons, the local pH within the resorbing cavities gradually becomes acidic and inorganic components such as the hydroxyapatite are dissolved. The concentration of calcium ions rises as the hydroxyapatite is dissolved over time. The concentration increases to a point at which calcium ions enter the osteoclasts through the membrane, inhibiting the osteoclast activity (54) and inducing the osteoclast apoptosis (55, 56). The decreased production of protons leads to a lower level of bone resorption and extracellular matrix digestion. Eventually, the osteoclasts detach and migrate away from the resorption cavities or undergo apoptosis (57).

2.2.2 Bone Remodeling

During bone remodeling, osteoclasts and osteoblasts work together to maintain bone tissue homeostasis by balancing the bone resorption by osteoclasts and the bone formation by osteoblasts. Over the span of one's life, bone tissue is under constant remodeling orchestrated by signaling pathways and cellular activities. This process can be recognized in the following five phases: quiescence, activation, resorption, reversal, and formation/mineralization (58) [Figure 5]. In the quiescent phase, bone cells rest on the bone surfaces in a flat and thin morphology, known as bone lining cells. Approximately 80% of cancellous bone surface and 95% of cortical bone surface are in quiescence in terms of bone remodeling (59). Processes extending from the bone lining cells reach into canaliculi and form connections with the network of osteocytes. Bone lining cells are involved in the maintenance of the bone fluid environment of ion fluxes and mineral homeostasis (60).

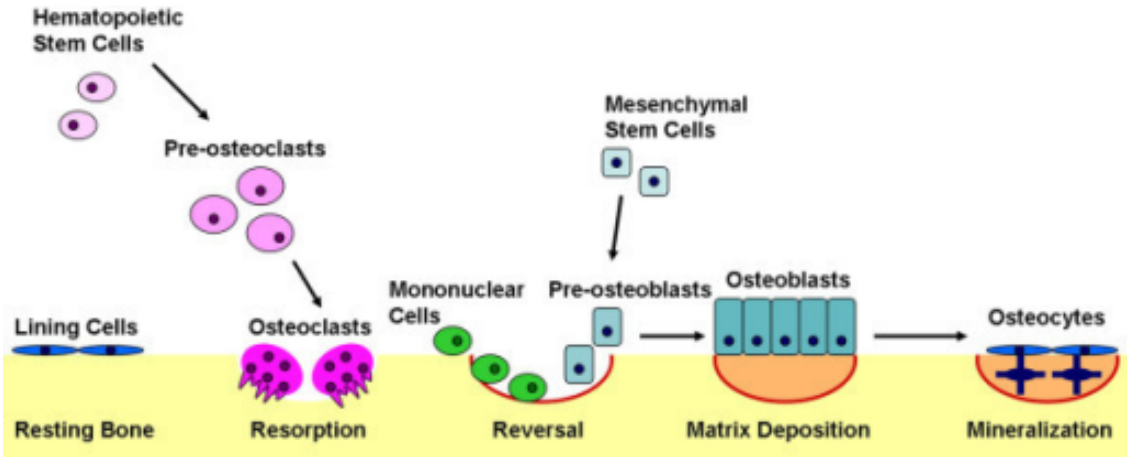

Figure 5. Schematic diagram of bone remodeling. (58, open access)

When the bone surface is activated, bone lining cells alter their morphology from being elongated and flat to one that is round and osteoblastic, and also become migratory (61). The critical step of the activation phase is the recruitment of mononuclear osteoclast progenitors, which differentiate and fuse into mature multinucleated osteoclasts after interacting with osteoblast progenitor cells and mature osteoblasts (62). The mature osteoclasts attach to the bone surface and start the resorption phase by producing enzymes and protons to decompose the organic component and dissolve the inorganic component (53). This process is also promoted by macrophages (63, 64) and factors released from the digested extracellular matrix such as platelet-derived growth factor (PDGF), insulin-like growth factor 1 (IGF-1) and transforming growth factor beta (TGF-beta) (65). The entire resorption phase of the remodeling cycle continues for two to three weeks. The transition phase between resorption and bone formation is referred to as the reversal phase. At the end of the resorption phase, a variety of cells are present at the resorption cavity sites, including

monocytes, osteocytes that are liberated from the bone matrix, and osteoclasts that are undergoing apoptosis. Osteoblast progenitors also migrate to the resorption sites so as to begin the process of bone formation (44). The coupling signal pathways that regulate the reversal phase are complex (66) and beyond the scope of this thesis. However, it is believed that some growth factors released from the matrix by resorption, such as insulin-like growth factors (IGF) and bone morphogenetic proteins (BMPs), promote the osteoblastic activities and bone formation (67). The osteoclasts are replaced with differentiated osteoblasts or pre-osteoblasts once the resorption phase is completed. It usually takes around five to ten days to generate the first layer of bone matrix by the osteoblasts and eventually the osteoid matrix is mineralized. The osteoblasts transform to bone lining cells that cover the surface of the regenerated bone tissue and establish the connection with osteocytes with the extended membrane process network. The transformation from osteoblasts to bone lining cells marks the end of the formation/mineralization phase and the beginning of the quiescent phase (the next remodeling cycle) (59).

2.2.3 Osteogenic Differentiation

Osteoblasts arise from the osteogenic differentiation of mesenchymal stem cells (MSCs) (68). MSCs are defined by the minimal criteria established by the International Society for Cellular Therapy (69), which are the positive expression of CD73, CD90 and CD105 surface markers; the negative expression of CD45, CD34, CD14 or CD11b, CD79-alpha or CD19 and human leukocyte antigen-D related (HLA-DR); attachment to tissue culture polystyrene surfaces, and the ability to differentiate towards osteoblasts, chondrocytes, and adipocytes *in vitro.* The differentiation process from MSCs to mature

osteoblasts includes four stages: mesenchymal cells, pre-osteoblasts, mature osteoblasts and eventually osteocytes (68).

During osteogenic differentiation, runt-related transcription factor 2 (Runx2) and transcription factor Osterix play important roles. Runx2 is believed to play a master regulating role in the entire osteoblastic differentiation process. In Runx2 knock-out mice, a cartilaginous skeleton was formed, but there was no presence of minerals or mineralization. The osteoblasts isolated from these mice showed an inability to initiate mineralization (70). Runx2 is critical in the differentiation both from MSCs to pre-osteoblasts and from pre-osteoblasts to mature osteoblasts, and it is mainly expressed by pre-osteoblasts and is down-regulated once pre-osteoblasts are differentiated into mature osteoblasts (71). Osterix also plays important roles and is needed for proper bone formation. Osterix is located downstream of Runx2, as indicated by a study where Runx2 was expressed in an animal model where the Osterix was knocked out, whereas Osterix was absent in the Runx2 knockout animal (72). Runx2 and Osterix are widely used as markers of osteogenic differentiation of MSCs and since the expression of Runx2 occurs throughout the early stage to the maturation of osteoblasts, Runx2 is also widely used as a marker of early osteogenic commitment of MSCs (71). The enzyme alkaline phosphatase (ALP) is commonly assessed as an early osteogenic differentiation marker (73). ALP plays a critical role in the mineralization of bone formation and an increased expression level of ALP is required for bone regeneration (74). The expression level of ALP elevates as the differentiation of pre-osteoblasts to mature osteoblasts occurs and gradually drops as osteoblasts differentiate into osteocytes or undergo cell death (75). At the stage of mature

osteoblasts, a high level of expression of alkaline phosphatase (ALP), osteocalcin (OC) and bone sialoprotein (BSP) is observed (76). Bone sialoprotein and osteocalcin are non-collagenous proteins secreted in the osteoid and are involved in the bone matrix mineralization. Bone sialoprotein binds to the collagen I secreted by the pre-osteoblasts and the osteoblasts, and the binding sites become nucleation sites of hydroxyapatite crystals (77). Osteocalcin is the most abundant non-collagenous protein secreted specially by osteoblasts and it has important roles in both bone formation and bone resorption (78, 79).

The selection of markers to assess the osteogenic differentiation varies according to the different stages of differentiation on which the study focuses, and the span of the differentiation that the study covers. For instance, the elevation of Runx2 occurs after the osteogenic commitment, and the expression of Runx2 stays at a relatively high level throughout the MSCs, pre-osteoblast and osteoblast stages, whereas osteocalcin is the specific marker that is used to indicate the presence of osteoblasts (68, 76) [Figure 6].

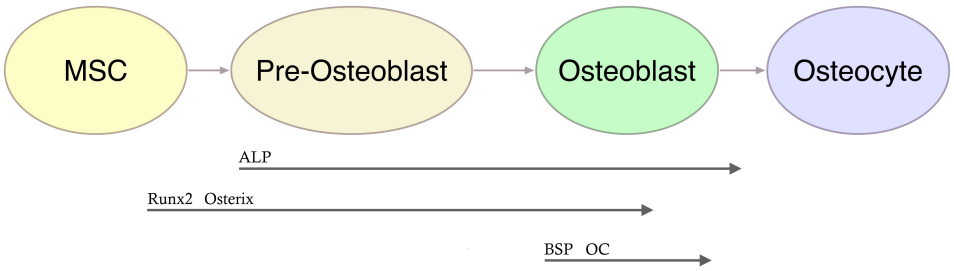

Figure 6. Diagram of the process of osteogenic differentiation and osteogenic markers at different phases. Runx2 and Osterix play important roles throughout the early differentiation and the maturation of osteoblasts. ALP expression starts to elevate once the MSCs are committed towards a osteogenic differentiation. BSP and osteocalcin are secreted by osteoblasts into the ECM, which are used as markers to indicate the formation of mature osteoblasts.

2.3 Fracture Healing

The process of healing and recovery that occurs after two vertebrae are fused into one after spinal fusion surgery is very similar to the way in which other bone fractures heal. The biological processes of spinal fusion are composed of the following three phases: the inflammation phase, the reparative phase and the remodeling phase [Figure 7] (80, 81) . There is no strict boundary between each phase throughout the entire healing process with different phases transitioning into the next and often overlapping each other for a period of time.

Inflammation occurs rapidly after the fusion surgery. As a result of the surgical trauma (e.g., damage to the blood supply, decortication of bone), a hematoma forms and

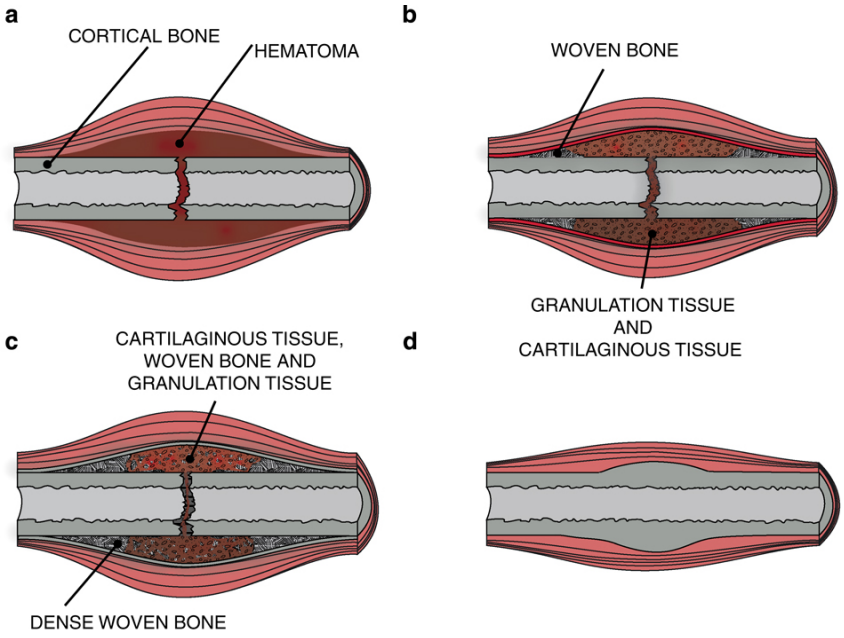

Figure 7. Fracture healing stages. a) Inflammation phase, characterized by the formation of hematoma. b) Early reparative phase, granulation tissue and cartilage tissue start to form and the woven bone tissue is generated. c) Late reparative phase, granulation tissue volume decreases, cartilage tissue starts to mineralize. d) Remodelling phase. (81, used with permission)

this region is soon invaded by inflammatory cells such as macrophages, blood monocytes and polymorphonuclear leukocytes (82). During the first few days after surgery, growth factors such as platelet-derived growth factor (PDGF), tumour necrosis factor alpha (TNF-alpha) and transforming growth factor beta (TGF-beta) and cytokines such as interleukin-1 (IL-1) and interleukin-6 (IL-6) are produced in order to regulate inflammatory responses and cellular activities, and to recruit mesenchymal stem cells from bone marrow and periosteum tissue to the fusion site (83). Angiogenesis is also initiated and stimulated by the growth factors and cytokines released around the wound site (82), and the hematoma is then gradually infiltrated and eventually replaced by fibrovascular tissue. This fibrovascular tissue, which is commonly referred to as a granuloma, serves as the scaffold for cell migration and the future woven bone formation (84).

The late period of the inflammatory phase overlaps with the reparative phase. The reparative phase begins 3-5 days after surgery and lasts for several weeks, during which vascularization is further increased, necrotic tissue is resorbed and a soft callus is formed by osteoblasts, chondroblasts and fibroblasts. These cells are differentiated from mesenchymal stem cells, which originate from the bone marrow and periosteum adjacent to the surgery sites or migrate to the surgery site through blood vessels. In the reparative phase, the tissue at the injury sites transforms from granulation tissue to a mixture of connective tissue, woven bone and cartilage and eventually only woven bone. This woven bone tissue bridges the vertebrae and becomes the scaffold for lamellar bone formation. Eventually, the woven bone tissue is replaced with lamellar bone by bone remodeling (85).

This transformation from granulation tissue to woven bone tissue is largely attributed to intramembranous ossification, cartilage formation and endochondral ossification. During intramembranous ossification, no cartilage is formed at the matrix of ossification as a precursor, but woven bone tissue is laid down directly by the osteoblasts differentiated from pluripotent mesenchymal cells or osteoblasts migrated from adjacent areas. This woven bone area is also referred to as a hard callus (86). As intramembranous ossification occurs, chondroblasts start to form cartilage at the central region of the fusion. Fibroblasts also form fibrous tissue in addition to the cartilage formation, and the combination of these two tissues is commonly referred to as a soft callus. The soft callus is eventually replaced so that in the end, only cartilage remains. In the late period of the reparative phase, chondroblasts stop producing collagens and transform into hypertrophic chondrocytes producing alkaline phosphatase which helps promote calcification of the cartilage. The cartilage then undergoes endochondral ossification and eventually it is replaced by the woven bone (85). During endochondral ossification, capillaries from the periosteum and nearby undamaged bone tissue begin to permeate the calcifying matrix and supply the matrix with oxygen and nutrients, as well as remove cellular wastes. With a more hospitable microenvironment created by the flow of nutrient and oxygen, osteoblasts also take up residence in the injured area and secrete osteoid, which will be remodeled into trabecular bones afterward (86) [Figure 8].

The final step of the bone healing process is the remodeling phase wherein the woven bone is replaced with lamellar bone. The remodeling process gradually modifies the distribution of lamellar bone in response to the stress load at the fusion site until an optimal

formation is achieved (44). In an animal model study, the formation of the cortical rim around the fusion site and the presence of newly formed bone marrow were also found, indicating the sophistication of this remodeling process (87).

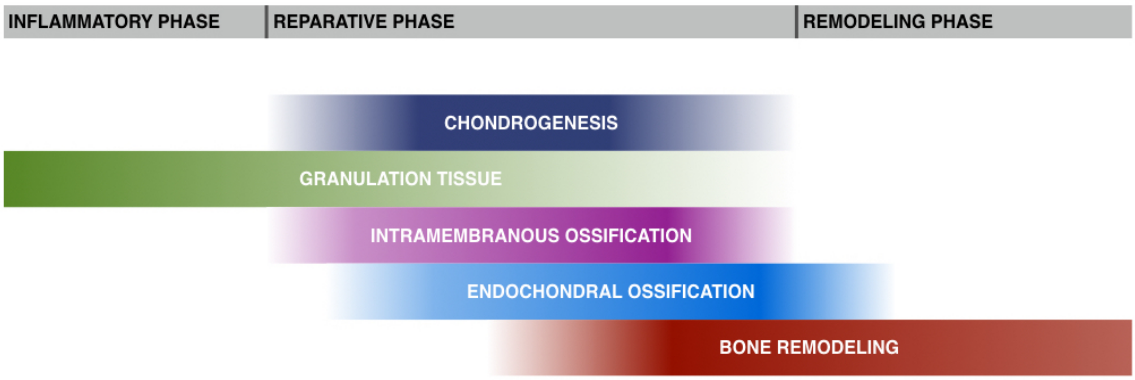

Figure 8. Timeline of bone fracture healing.

2.4 BCSPs

There are three essential design criteria for a successful bone graft in the post-surgery healing process of spinal fusion: the capability of osteogenesis, and the ability to be osteoconductive and osteoinductive (88). The osteogenesis criterion means that the graft should include osteogenic cells or precursors and is able to generate bone tissue *in situ*. The osteoconductive agent serves as a scaffold to which the osteo-related cells can attach, migrate towards, and grow on or serves as a factor to regulate cell attachment and migration. It supports the bone ingrowth and facilities fusion site revascularization. Osteoinductive factors are able to initiate or promote osteogenic differentiation of

osteoprogenitors, improve the proliferation of the osteo-related cells or to recruit cells to the fracture sites to aid the fusion process (89).

BCSPs are synthetic peptide fragments selected from the alpha I chain of the human Type I collagen [Figure 9]. The amino acid sequences of BCSP1, BCSP7, and BCSP11 are Asn-Gly-Leu-Pro- Gly-Pro-Ile-Gly-hydroxy Pro, Pro-Gly-Pro-Ile-Gly and Gly-Pro-Ile-Gly, respectively. In a previous in vivo study (90), BCSP1 and BCSP7 were administrated onto the periosteum tissue at the tibia of rabbit, and after 7 days the bone mineral content (BMC) and bone mineral density (BMD) at the injection sites [region 2 in Figure 10] and whole tibia were measured. Scan results showed that, at the injection region and the whole tibia, both bone mineral content and bone mineral density were significantly

Collagen I alpha-1 chain, Human	MFSFVDLRLLLLLAATALLTHGQEEGQVEGQDEDIPPITCVQNGLRYHDRDVWKPEPCRICVCDNGKVLC DDVICDETKNCPGAEVPEGECCPVCPDGSESPTDQETTGVEGPKGDTGPRGPRGPAGPPGRDGIPGQPG LPGPPGPPGPPGPPGLGGNFAPQLSYGYDEKSTGGISVPGPMGPSGPRGLPGPPGAPGPQGFQGPPGEPGE PGASGPMGPRGPPGPPGKNGDDGEAGKPGRPGERGPPGPQGARGLPGTAGLPGMKGHRGFSGLDGAK GDAGPAGPKGEPGSPGENGAPGQMGPRGLPGERGRPGAPGPAGARGNDGATGAAGPPGPTGPAGPPGF PGAVGAKGEAGPQGPRGSEGPQGVRGEPGPPGPAGAAGPAGNPGADGQPGAKGANGAPGIAGAPGFPG ARGPSGPQGPGGPPGPKGNSGEPGAPGSKGDTGAKGEPGPVGVQGPPGPAGEEGKRGARGEPGPTGLPG PPGERGGPGSRGFPGADGVAGPKGPAGERGSPGPAGPKGSPGEAGRPGEAGLPGAKGLTGSPGSPGPDGK TGPPGPAGQDGRPGPPGPPGARGQAGVMGFPGPKGAAGEPGKAGERGVPGPPGAVGPAGKDGEAGAQG PPGPAGPAGERGEQGPAGSPGFQGLPGPAGPPGEAGKPGEQGVPGDLGAPGPSGARGERGFPGERGVQG PPGPAGPRGANGAPGNDGAKGDAGAPGAPGSQGAPGLQGMPGERGAAGLPGPKGDRGDAGPKGADGS PGKDGVRGLTGPIGPPGPAGAPGDKGESGPSGPAGPTGARGAPGDRGEPGPPGPAGFAGPPGADGQPGA KGEPGDAGAKGDAGPPGPAGPAGPPGPIGNVGAPGAKGARGSAGPPGATGFPGAAGRVGPPGPSGNAGP PGPPGPAGKEGGKGPRGETGPAGRPGEVGPPGPPGPAGEKGSPGADGPAGAPGTPGPQGIAGQRGVVGLP GQRGERGFPGLPGPSGEPGKQGPSGASGERGPPGPMGPPGLAGPPGESGREGAPGAEGSPGRDGSPGAK GDRGETGPAGPPGAPGAPGAPGPVGPAGKSGDRGETGPAGPTGPVGPVGARGPAGPQGPRGDKGETGE QGDRGIKGHRGFSGLQGPPGPPGSPGEQGPSGASGPAGPRGPPGSAGAPGKDGL **NGLPGPIGP**PGPRGRTGDAGPVGPPGPPGPPGPPSAGFDFSFLPQPPQEKAHDGGRYYRADDANVVR DRDLEVDTTLKSLSQQIENIRSPEGSRKNPARTCRDLKMCHSDWKSGEYWIDPNQGCNLDAIKVFCNMET GETCVYPTQPSVAQKNWYISKNPKDKRHVWFGESMTDGFQFEYGGQGSDPADVAIQLTFLRLMSTEASQ NITYHCKNSVAYMDQQTGNLKKALLLQGSNEIEIRAEGNSRFTYSVTVDGCTSHTGAWGKTVIEYKTTKT SRLPIIDVAPLDVGAPDQEFGFDVGPVCFL
BCSP1	PGSAGAPGKDGL**NGLPGPIGP**PGPRGRTGDAGPVG
BCSP7	PGSAGAPGKDGLNGL**PGPIG**PPGPRGRTGDAGPVG
BCSP11	PGSAGAPGKDGLNGLP**GPIG**PPGPRGRTGDAGPVG

Figure 9. BCSP sequence and its location in human collagen I peptide sequence.

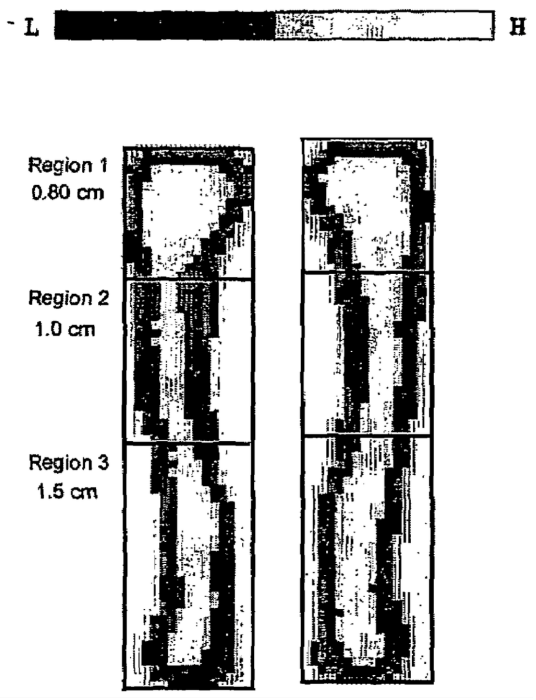

Figure 10. Bone densitometry analysis of the BCSP treated tibia. The BMC increase and BMD increase of the whole tibia were analyzed on all three regions. BMC increase and BMD increase around the injection sites were analyzed at region 2. "L" and "H" indicate low density and high density of the bone mass. More high density bone mass was observed on the tibia scan image on the left (BCSP1 treated) compared to the non BCSP treated group on the right. (87)

greater in the BCSP-treated groups as compared to the controls [Figure 11]. BCSP11 was not assessed *in vivo* but an *in vitro* study was conducted to assess its osteogenic promoting capability [personal communication from Dr. Tim Smith, Octane]. The RNA expression levels of various osteogenic markers, such as osteopontin, BMP-2 and BSP, were significantly elevated after the treatment with BCSP11 in the concentrations range from 0.1 ng/mL to 100 ng/mL over a period of three weeks, which was indicated by at least a 2.5-fold increase of RNA expression compared to the non BCSP11 treated controls. A previous *in vitro* study also indicated that BCSP1 had a dose dependent stimulating effect on the proliferation of bovine chondrocytes, human chondrocytes, and rat bone marrow derived osteoblasts (90).

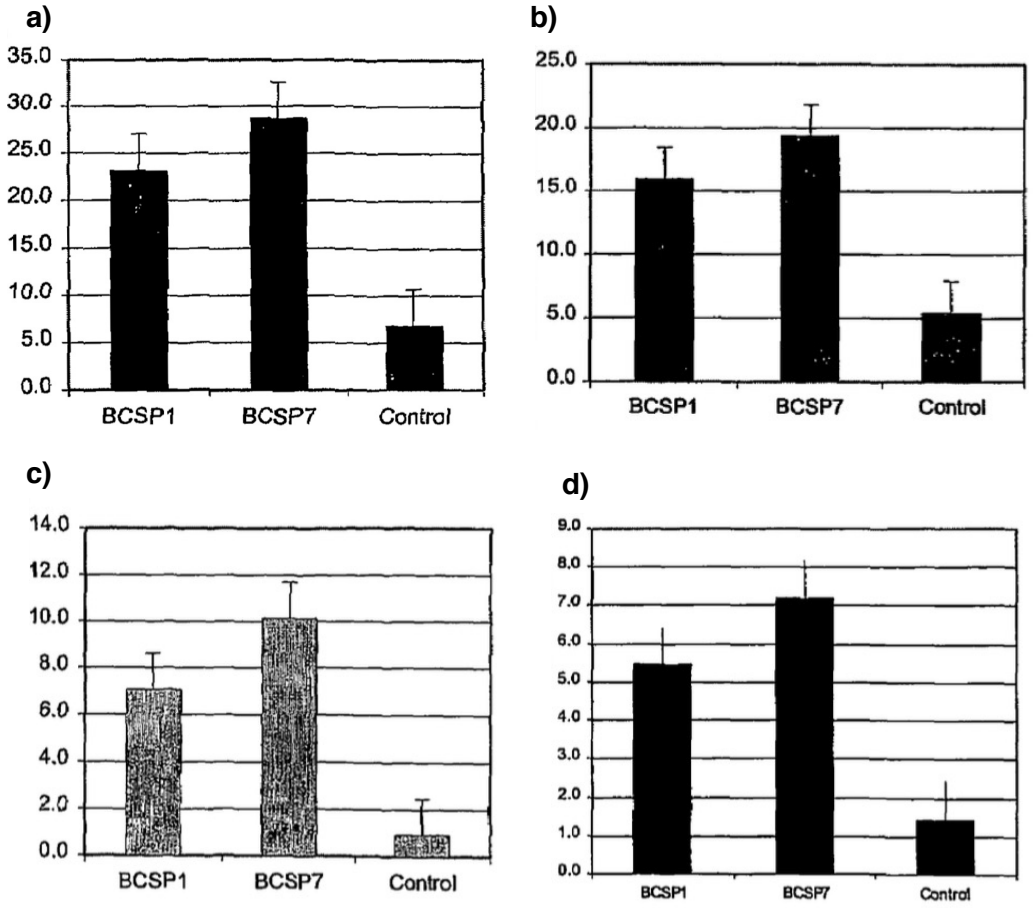

Figure 11. Bone mass content (BMC) and bone mass density (BMD) scan results 7 days after the treatment of BCSP1 and BCSP7 in the *in vivo* study. a) BMC percentage of increase at region 2. b) BMD percentage of increase at region 2. c) BMC percentage of increase in the whole tibia. d) BMD percentage of increase in the whole tibia. Treatment of BCSP1 or BCSP7 significantly enhanced the bone mass content increase and bone mass density increase around the injection sites (region 2) and in the whole tibia compared to the non-BCSP treated group (Control). (87, adapted)

2.5 Experiment Cell Types

2.5.1 MC3T3-E1 Preosteoblasts

The MC3T3-E1 cell, with its pre-osteoblastic phenotype, has been the most commonly used cell line for *in vitro* osteogenesis studies since its establishment from the newborn mouse calvaria (91). A high ALP expression level was used as a biological

parameter for MC3T3-E1 cell selection. Sub-clones of this cell line were further characterized by their mineralization capability and late osteogenic marker expression of proteins such as bone sialoprotein (92). MC3T3-E1 cells demonstrate a mineralization process that is very similar to that of intramembranous ossification *in vivo* (91). Sub-clones 4, 8, 11, 14 and 26 stained positive for the presence of mineralization using a Von Kossa stain, after being cultured in an inorganic phosphate and ascorbic acid supplemented medium. Sub-clones 4 and 14 demonstrated collagen-associated mineralization with the characteristic fibrillar Von Kossa staining, whereas sub-clone 17 and 24 culture showed the characteristic granular mineralization of ectopic mineral that is non-collagen associated. The MC3T3-E1 subclone 4 is an effective cell source to study bone biology and it was used in this study for its consistency of cell performance (mineralization, osteogenic marker expression, etc.) throughout previous studies (93-96) and because there are well established techniques to detect its osteogenic process (ALP level increase and decrease, mineral formation, etc.). The ability of BCSPs to affect MC3T3-E1 sub-clone 4 proliferation, differentiation, mineralization and migration were assessed with various concentrations.

2.4.2 Human BM-MSCs

Human BM-MSCs are a widely studied and used cell type in bone regeneration and fracture healing and represent a gold standard to compare with in terms of osteogenic differentiation and osteogenesis (97-99). The proliferation (cell growth) and differentiation (towards osteoblastic cells or chondrogenic cells) of BM-MSCs are crucial to bone tissue regeneration and the outcome of the fracture repair. The enhancement of the bio-activities of BM-MSCs by a stimulating agent can make this agent a promising candidate for post-

surgical drug administration. Recently, utilizing the clinical benefits of mesenchymal stem cells has emerged as a new strategy to assist the fracture healing process (100, 101). Osteoprogenitors are isolated from bone marrow and expanded *ex vivo*, prior to the *in vivo* application via scaffolds (100, 102). Stem cell therapy could potentially benefit from the improvement of BM-MSC osteogenic activities during *ex vivo* cell expansion (103, 104). In this present study, the effects of BCSPs were assessed with respect to proliferation stimulating, differentiation inducing, and mineralization stimulating on human BM-MSCs *in vitro*.

2.4.3 Periosteum Derived Stem Cells

Periosteum possesses a composite structure with two main layers. The outer layer is a thick and fibrous layer that consists of two sections. The superficial zone of the outer layer contains a large amount of organized collagen fibres and elastic fibres as well as a small amount of matrix, cells and blood vessels. The layer beneath this fibroelastic layer is known as the matrix layer, which is highly vascularized and contains a relatively large amount of collagenous matrix. Some of these blood vessels extend through the periosteum into the cortical bone and form a blood supply network with blood vessels in the osteons. The inner layer, which is commonly referred to as the cambium layer, is relatively thin and is the cell reservoir of the periosteum tissue, containing cells that are either fibroblastic, osteoblastic, or other cells that still maintain the multi potential (105).

Cells isolated from the periosteum tissue are commonly referred to as periosteal cells or periosteum derived cells. Osteoblast-like cells represent about 90% of cells in the cambium layer, whereas fibroblast-like cells make up around 95% of the cells in the

fibroelastic layer (106). The density of fibroblast-like cells increases moving from the cambium layer that is close to the bone surfaces to the outer fibroelastic layer. The morphology also changes from a round shape to a flat and elongated shape towards the outer layer of periosteum. The cell population of the periosteum tissue is composed of MSCs, fibroblasts, osteoblasts and pericytes. In addition to a significant portion of the cell population that is recognized as MSCs, the osteocytes and fibroblasts also exhibit very similar morphology and differentiation potential to that of MSCs (107, 108). The distinction that can specifically separate fibroblast-like multi-potential cells apart from fibroblasts in the periosteum tissue remains poorly studied. However, a comparison study using a rabbit model presented evidence that cells derived from the cambium layers showed a higher osteogenic phenotype than cells derived from the fibroelastic layer, by producing a higher level of alkaline phosphatase and osteocalcin (109). Studies have also shown that periosteum derived cells have comparable osteogenic ability, if not better, to that of human BM-MSCs in bone regeneration (110-112).

In the *in vivo* bone regeneration study by Stevens, M. M. et al., space was created *in vivo* between the cortical bone surface and periosteum tissue, which was filled with the injection of a calcium-alginate gel in the absence of growth factors, and this approach was to trigger a fracture healing response to the "gap" created between periosteum tissue and the bone surface. A series of osteogenic behaviours were observed in the space and new bone tissue was generated over 12 weeks; periosteal cells and newly generated capillaries filled the space at day 3, woven bone tissue was observed after 2 weeks and bone remodeling was observed with the decrease of woven bone tissue and the increase of lamellar bone tissue 8

weeks after the space manipulation (113). In the *in vivo* rabbit model study with BCSPs described previously, bone mass content and bone mass density were increased significantly when BCSPs were administrated onto the periosteum tissue of intact tibia, and the majority of the bone mass content increase and bone mass density increase occurred around the BCSP injection sites. These findings indicated that periosteum and cells migrated from the periosteum play important roles in fracture healing and periosteum-derived cells could be one of the cell types that are responsive to BCSPs. In the present study, the potential stimulating effect of BCSPs on cell proliferation and cell migration were examined with periosteum-derived stem cells isolated from rabbits (rPDSCs) and human PDSCs obtained from Octane Inc.

2.6 Scope and Objective

BCSPs appear to promote bone growth *in vivo* and the osteogenic process *in vitro* as described above. BCSPs therefore have the potential to be used as osteoinductive factors in a bone graft system to enhance the bone growth and fusion process. The long-term objective of this research project involves assessing the cellular and molecular mechanisms of BCSPs' performance, developing a drug delivery system for a controlled dosage of BCSPs, integration of BCSPs and the delivery system and assessment of its biocompatibility, stability, and overall performance. For this thesis, the objective was to screen three BCSPs in various concentrations with respect to their ability to enhance proliferation, to induce early osteogenic differentiation and mineralization, and to simulate the migration of osteoprogenitor cells *in vitro*.

2.7 Approach

The stimulating effects of each of BCSP1, BCSP7 and BCSP11 on proliferation, early osteogenic marker expression and cell culture mineralization were first screened with MC3T3-E1 preosteoblasts and hBM-MSCs. Given the significance of the periosteum tissue to bone fracture healing as described above, the enhancement of the performance of periosteal cells is a promising direction to study in order to optimize the healing process. Promoting cell migration to the fracture or surgery sites is one of the strategies for increasing the population of clinically useful cells such as osteogenic cells and cells with osteogenic potential. The screening of the stimulating effects of BCSPs was carried on hPDSCs with the assessments of the stimulating effect of BCSP1, BCSP7 and BCSP11 on hPDSC proliferation, and migration. Assessment of the stimulating effect of BCSP1 on rabbit PDSC migration was also carried out in an effort to confirm the reported *in vivo* bone growth stimulating effect of BCSP1 in a rabbit model. Migration assays of BCSP1, BCSP7 and BCSP11 were also carried out with MC3T3-E1 preosteoblasts. Experiment conditions and time points were listed below [Table 1].

Table 1. Conditions and time-points in BCSP assessment assays.

The concentrations indicate the experiment conditions in each assay (e.g., the proliferation assay of MC3T3-E1 was carried out after the treatment of BCSP1, 7 or 11 at the concentration of 10 or 50 ng/mL)

Aspects		Proliferation	Differentiation	Mineralization	Migration
Methods		dsDNA quantification	ALP expression assay	Alizarin Red S staining	Boyden Chamber assay
Cell types	MC3T3-E1	10, 50 ng/mL	10, 50 ng/mL	10, 50 ng/mL	10, 25, 50 ng/mL
	hBM-MSCs	10, 50 ng/mL	10, 50 ng/mL	10, 50 ng/mL	
	hPDSCs	10, 25, 50 ng/mL			10, 25, 50 ng/mL
	rPDSCs				BCSP1 at 10, 25, 50 ng/mL)

The assays were conducted at the time points listed below. (e.g., proliferation assay with hBM-MSCs was conducted with a dsDNA quantification after 5 days of BCSP treatment)

Cell types	MC3T3-E1	Day 5	Day 7	Day 14	24 hrs
	hBM-MSCs	Day 5	Day 14	Day 21	
	hPDSCs	Day 5			24 hrs
	rPDSCs				24 hrs (BCSP1 only)

Chapter 3: Materials and Methodology

3.1 Cell Sources and Materials

MC3T3-E1 subclone 4 preosteoblast cells and human bone marrow-derived mesenchymal stem cells (hBM-MSCs) were obtained from ATCC (Manassas, VA, USA). Rabbit periosteum-derived stem cells (rPDSCs) were isolated from the tibia of fresh rabbit cadavers. Human periosteum-derived stem cells (hPDSCs) were obtained from Octane Biotech Inc (Kingston, ON, Canada). Basal medium for hBM-MSC was Dulbecco's Modified Eagle Medium (DMEM) with low glucose (SH30021.FS, GE Healthcare Life Sciences) and basal medium for MC3T3-E1 was MEM Alpha Modification (alpha-MEM, SH30265.01, GE Healthcare Life Sciences). A 1:1 mixture of DMEM and Ham's F12 medium (DMEM-F12) was used as the basal medium for both rPDSC and hPDSC culture.

BCSP1, BCSP7, BCSP11 were obtained from Octane Biotech Inc. (Kingston, ON, Canada). Sodium chloride (NaCl), magnesium chloride ($MgCl_2$), Nuclear Fast Red, tris(hydroxymethyl)aminomethane hydrochloride (Tris-Cl), ethylenediaminetetraacetic acid (EDTA), TritonX-100, aluminum sulfate, dexamethasone, ascorbic acid-2-phosphate, beta-glycerophosphate, bovine serum albumin (BSA), silver nitrate and paraformaldehyde were purchased from Sigma-Aldrich Canada Co. (Oakville, Ontario). Fetal bovine serum (FBS), penicillin-streptomycin (pen-strep), 0.25% trypsin-EDTA were obtained from Life Technologies Inc. (Burlington, Ontario). P-nitrophenyl (pNP) and Alizarin Red S were purchased from MP Biomedicals, LLC. (Santa Ana, USA). Collagenase type II was purchased from Worthington Biochemical Co. (Lakewood, New Jersey). 4',6-diamidino-2-

phenylindole (DAPI) mounting medium was obtained from Abcam (Cambridge, Massachusetts). Dimethyl sulfoxide (DMSO) was purchased from Corning Cellgro (Manassas, USA).

3.2 Cell Culture

3.2.1 MC3T3-E1 preosteoblast primary expanding culture

Cells from ATCC (Manassas, VA, USA) were thawed from the vial and seeded in T175 flasks at a density of 3,000 cell/cm^2. Alpha-MEM supplemented with 10% FBS and 1% pen-strep were used as complete medium with the medium being changed every two days. Once the cell population reached approximately 90% confluence, the cells were subcultured and propagated for future experiments. The medium was removed and cells were rinsed with PBS twice, and then 25 mL of trypsin-ethylenediaminetetraacetic acid (trypsin-EDTA) was added to each T175 flask. Flasks were incubated at 37°C for 3-5 min and observed under an inverted microscope to ensure proper cell dispersion. Cell solutions were then transferred to 50 mL Falcon tubes and the same amount of complete growth medium was added to the tube to stop the trypsinization. Finally, cells were collected via centrifugation at 500g for 5 min and resuspended in complete growth medium for cell counting and subculturing. Appropriate aliquots of the cell solution were transferred to new T175 flasks at a density of 3,000 cell/cm^2. Subculture was carried out twice and cells were cryopreserved for future experiments. Passage 3 cells were used in the experiments.

3.2.2 hBM-MSCs primary expanding culture

Cells purchased were thawed and seeded at a density of 5,000 cell/cm^2 in a T175 flask. In primary expanding culture, the Mesenchymal Stem Cell Growth for Bone Marrow-derived MSCs (PCS-500-041, ATCC) was used as basal medium, supplemented with Mesenchymal Stem Cell Growth Kit for Bone Marrow-derived MSCs (PCS-500-041, ATCC) (final concentration: 7% FBS, 15 ng/mL rh-IGF-1, 125 pg/mL rh-FGF-b) and 1% pen-strep with the medium being changed every two to three days. When the cell population was approximately 90% confluent, the medium was removed and the cells were rinsed with PBS twice. 25 mL of trypsin-EDTA was added to the T175 flask and the flask was incubated at 37°C for 3-5 min. The flask was observed under an inverted microscope for proper cell dispersion. Cell solutions were then transferred to 50 mL falcon tubes and same amount of complete growth medium was added to the tube to stop the trypsin-EDTA. Finally, cells were centrifuged at 500 g for 5 min and then resuspended in complete growth medium for cell count and following subculture. Appropriate aliquots of the cell solution were transferred to new T175 flasks at a density of 5,000 cell/cm^2. Subculture was carried out twice and the cells were cryopreserved for future experiments.

3.2.3 Rabbit Periosteum Derived Stem Cells Isolation

Periosteum tissues were isolated from the medial proximal tibia of a male New Zealand dwarf rabbit in 0.5 cm × 0.5 cm squares and these fragments were washed twice with PBS with 1% pen-strep. The periosteum fragments were digested in DMEM-F12 (supplemented with 10% FBS and 1% pen-strep) with 0.25 % collagenase type II (CLS-2, Worthington, Freehold, NJ, #LS004176) for 4 h at 37°C. The digested cell solution was

filtered through a 40 μm cell strainer (Fisher, #22-363-547) and the cells were collected via centrifugation at 500g for 10 min. Primary cells were resuspended in the T175 flask and cultured to around 90% confluence before the subculture was carried out. For the subculture, 25 mL trypsin-EDTA was added to the T175 flask and the flask was incubated at 37°C for 3-5 min. The cells were transferred to the 50 mL falcon tube once they were properly dispersed, and then centrifuged at 500g for 5 min. Cells were counted and transferred to new T175 flasks at a density of 5,000 cells/cm^2 to complete the subculture. Subculture was carried out twice and passage 3 cells were used in the experiments.

3.2.4 Osteogenic Differentiation Characterization

Human PDSCs were cultured in osteogenic medium for 21 days and isolated rabbit PDSCs were cultured in osteogenic medium for 14 days prior to the osteogenic differentiation characterization using Von Kossa staining. Osteogenic medium was prepared with complete medium and 10 mM beta-glycerophosphate, 10 nM dexamethasone, and 50 μg/mL ascorbic acid-2-phosphate. Briefly, the cells were washed with deionized water twice and fixed with 4% paraformaldehyde solution for 30 min. Fixed cells were again washed twice with deionized water and incubated with 5% silver nitrate solution under a UV light for 30-45 min (longer exposure was required if darker cell sheets were not observed). The cell sheets were washed with deionized water and un-reacted silver was washed by 5% sodium thiosulfate solution. Cell sheets were washed and then stained with 0.1% Nuclear Fast Red solution (0.1% Nuclear Fast Red with 5% aluminum sulfate). The mineral deposition, nuclei and cytoplasm were stained black/brown-black, red, and pink, respectively.

3.2.5 Cryopreservation

The same cryopreservation method were used for all cell types. Cells were detached from the flasks by adding 25 mL of trypsin-EDTA to T175 flasks or 10mL to T75 flasks and cultured for 3 to 5 min. Flasks were observed under a microscope and once the cells were properly dispersed, trypsinization was stopped by adding the same amount of complete medium. Cell number was counted with a hemacytometer, and the cells were collected via centrifugation at 500g for 5 min. The cryopreservation solution was 80% FBS, 10% complete culture medium and 10% DMSO. Collected cells were aliquoted in the cryopreservation vials at a density of 1.5 million cells/vial and preserved in liquid nitrogen.

3.3 Cell Proliferation Assay QuantiFluor® dsDNA Quantification:

MC3T3-E1 cells were seeded to 24-well plates at a density of 10,000 cells/well and cultured with complete growth medium (alpha-MEM supplemented with 10% FBS and 1% pen-strep). 24 h after initial seeding, the medium was changed to the complete growth medium supplement with BCSP1, BCSP7 and BCSP11 at the concentrations of both 10 ng/mL and 50 ng/mL. The BCSP supplemented medium was changed every two days and after 5 days of culture, a proliferation assay was carried out using a QuantiFluor® dsDNA Quantification kit (Promega, USA). Briefly, the cells were washed with PBS twice to remove serum proteins on the surface and then lysed in 1 mL lysis buffer (50 mM Tris-HCl, 150 mM NaCl, 1mM EDTA, 1% TritonX-100, adjusted to pH 8) to obtain the cell lysate solution. All samples were analyzed in duplicate in 96-well plates (Corning-Costar, Oneonta, USA). For each replicate, 100 μL cell lysate solution and 100 μL QuantiFluor® dsDNA Dye (1X) were

mixed and incubated for 5 min while protected from light at room temperature. The fluorescence was read at an excitation wavelength of 504 nm and emission wavelength of 531 nm with a plate reader (EnSpire Multimode Plate Reader, PerkinElmer Inc). Readings were converted to dsDNA concentration using a standard curve prepared according to the manufacturer's protocol and then converted to the total cell number with the total lysate solution volume of each well (1 mL) and a 6 pg dsDNA/cell ratio (114).

The proliferation of hBM-MSCs was analyzed 5 days after the initial seeding at 2,000 cells/well density. The proliferation assay of hPDSCs with BCSP1 was conducted 5 days after initial seeding at 3,000 cells/well. The proliferation assay of hPDSCs with BCSP7 and BCSP11 were conducted 5 days after initial seeding at 2,000 cells/well. All proliferation assays were carried out with the QuantiFluor® dsDNA Quantification kit (Promega, USA) to quantify the cell numbers.

3.4 Early Differentiation Marker Alkaline Phosphatase Assay

MC3T3-E1 cells were seeded in the 24-well plates at a density of 100,000 cells/well. 24 h after initial seeding, the complete medium was changed to BCSP supplemented medium. The medium was changed every 2 days and at day 7, the ALP expression level was analyzed with a p-nitrophenyl phosphate liquid substrate system (N7653, Sigma). Cells were gently washed twice with PBS and sonicated in 1 mL ALP buffer (100 mM NaCl, 5 mM MgCl2, 100 mM Tris-Cl, adjust to pH 9.5). The lysate solutions were transferred to 1.5 mL Eppendorf tubes and centrifuged at 13,000g for 10 min, and the supernatant was then collected for the assay. In the 96-well plates, 100 μL p-nitrophenyl phosphate substrate was

added to 40 μL of lysed sample solution, and 40 μL ALP buffer was used as a blank. Following 30 min of incubation at room temperature, the absorbance was measured at 405 nm with a plate reader. The blank reading was subtracted from the sample readings and the results were standardized to nmol pNP generated /min according to the standard curve prepared with p-nitrophenyl and further normalized to the nmol pNP/mg protein/min with the protein content measurement. The ALP/protein readings were also standardized to the control group result and presented as fold-increase of the ALP expression level over control after the treatment of various dosages of BCSPs.

Protein content was measured using the Bio-Rad Protein Assay. Briefly, 40 μL of Bio-Rad reagent was added to 100 μL of each lysed sample and 100 μL ALP buffer as blanks on the 96-well plates. The plates were incubated at room temperature for 5 min and the absorbances was measured at 595 nm by the plate reader. The blank reading was subtracted from the absorbance reading of each lysed sample and the results were standardized to mg protein according to the standard curve prepared with bovine serum albumin. The protein content results were used to normalize the ALP absorbance readings.

hBM-MSCs were seeded to the 24-well plates at a density of 60,000 cells/well. ALP assays were carried out after 14 days of treatment with BCSP1, BCSP7 and BCSP11 at the dosages of 10 ng/mL added every second day and 50 ng/mL added every second day.

3.5 Mineralization Alizarin Red S Staining Assay

MC3T3-E1 cells were seeded on 12-well plates in a 150,000 cells/well density. 24 h after initial seeding, the complete media were changed to fresh complete media as control,

to osteogenic medium (complete medium with 10 mM beta-glycerophosphate, 10 nM dexamethasone, and 50 μg/mL ascorbic acid-2-phosphate) as positive control, and to BCSP supplemented complete medium as experimental conditions. Culture medium was changed every two days and at day 14, Alizarin Red S staining was used to assess the mineral deposition qualitatively and quantitatively. Briefly, the medium was removed from each well and the cells were gently washed twice with Milli-Q water. Cells were fixed with paraformaldehyde solution (4%, pH 7.4) for 30 min at room temperature afterwards and washed with deionized water. Then, the cells were stained with the Alizarin Red S solution (40 mM, pH 4.1-4.2) at room temperature for 15 min and any un-bound dye was gently washed off with deionized water. Pictures of the culture plates of the experimental groups were taken using a photo scanner (Epson Perfection V600 Photo). Images of the positive control groups were taken with an inverted microscope to confirm the osteogenic characteristic of the cells. The dye extraction solution (20% methanol and 10% acetic acid) was added to each well and allowed to stay at room temperature for 15 min with gentle shaking. Dye solutions were collected in Eppendorf tubes from each well and transferred to 96-well plates (100 μL/well) in duplicate prior to the absorbance measurement at 450 nm with the plate reader. For hBM-MSCs, the mineralization assay was conducted on Day 21 after the initial seeding at 100,000 cells/well density with the same method used for MC3T3-E1 cell mineralization.

3.6 Migration Boyden Chamber Assay

Random cell movement regardless of the concentration of soluble factors is generally referred to as chemokinesis, whereas directed migration in response to the presence of a soluble stimulus, such as cytokines and growth factors, is known as chemotaxis. The migration assessment was carried out with a Boyden chamber assay (115), in which chemotactic agents were added to the bottom part of the chamber and cells are seeded at the top [Figure 12]. ThinCerts Cell Culture Inserts (8 µm pore size, Greiner Bio-One Inc., #662638) were placed in the 24-well plates. 600 µL of complete culture medium was added to the plate wells as control and 600 µL of BCSP supplemented medium (complete culture medium with BCSP in various concentrations) was added to the plate wells below the inserts as experimental conditions. 200 µL of cell solution was added into each insert. Cell culture plates with inserts were incubated at 37°C and 5 % CO_2 for 24 h. After 24 h, the inserts were gently washed three times with PBS. Non-migrated cells left

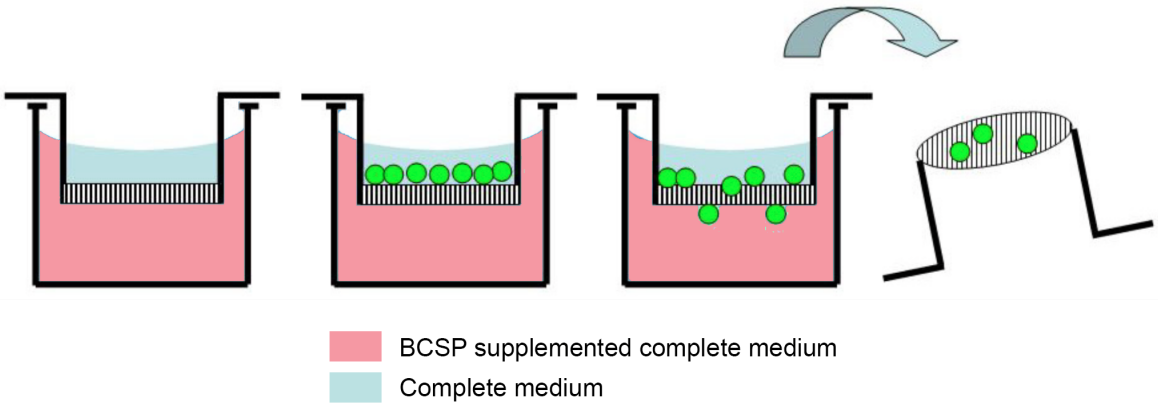

Figure 12. Diagram of chamber migration assay. Cells were seeded inside the inserts and BCSP supplemented medium was added outside the inserts in the wells. After 24 hours of culture, un-migrated cells in the inserts were removed and migrated cells were fixed, stained and counted afterwards. Adapted from (115, open access)

inside the inserts were removed with cotton swabs and the insert membranes were then fixed with 4% para-formaldehyde solution for 20 min at room temperature. The membranes were detached from the inserts and stained with 4′ 6-diamidino-2-phenylindole (DAPI), followed by fluorescent cell imaging using a confocal microscope (Olympus FV1000). The area of each image was 33.6 mm^2 and at least six pictures were taken at different locations for each membrane. The cell number on each picture was counted using ImageJ, and the cell migration percentage was then calculated with an equation of average cell number per picture, actual size of a single picture, size of the membrane culture surface and total number of seeded cell, as noted below.

$$Migration\ Percentage = \frac{(Average\ Cell\ Number\ per\ Picture) \times (Size\ of\ Membrane\ Surface)}{(Actual\ Size\ of\ One\ Picture) \times (Total\ Number\ of\ Seeded\ Cell)}$$

3.7 Statistics

Significant differences were assessed using a one-way ANOVA with a Tukey post-hoc test performed using Graphpad Prism 6 (Graphpad Software, La Jolla, CA, USA) and $p \leq 0.05$ was considered significant ("*"= $p<0.05$, "**"= $p<0.01$, "***"= $p<0.001$, "****"= $p<0.0001$). Data values are presented as means ± standard deviation (SD) and the number of samples per group (n) is indicated for each experiment.

Chapter 4: Results

4.1 Proliferation

No significant difference in cell numbers between each group was observed of either MC3T3-E1 pre-osteoblasts [Figure 13], hBM-MSCs [Figure 14] or hPDSCs [Figure 15] in the presence of any of the three BCSPs. During a 5 day exposure to BCSP1, BCSP7 and BCSP11, the growth of MC3T3-E1 pre-osteoblast cells, hBM-MSC and hPDSCs was not inhibited. However, the BCSPs also did not have a positive effect on the cell growth of these three types of cells.

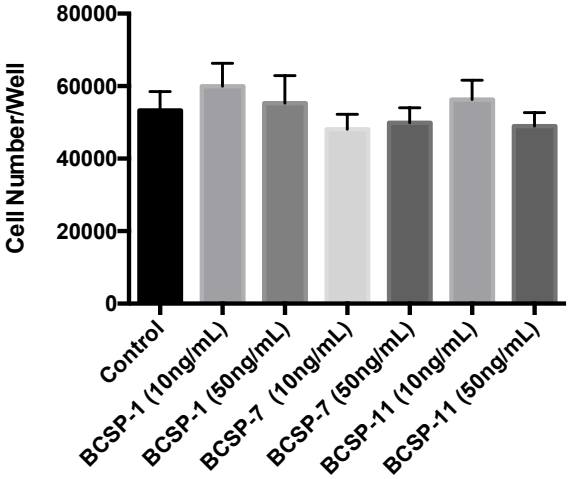

Figure 13. Proliferation assay result of MC3T3-E1 preosteoblast. The dsDNA quantification assay was conducted 5 days after initial cell seeding. Initial seeding density: 10,000 cells/well, n=6.

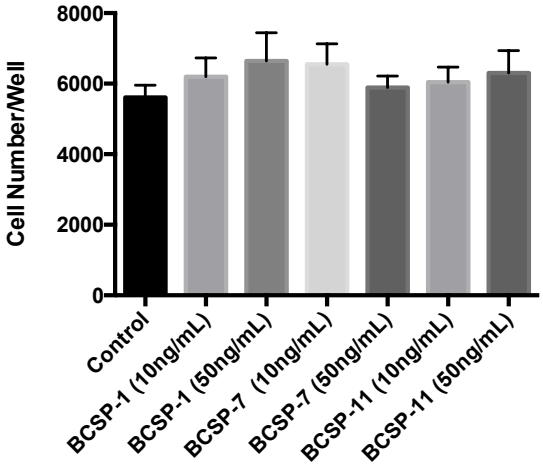

Figure 14. Proliferation assay result of human BM-MSCs. The dsDNA quantification assay was conducted 5 days after the initial cell seeding. Initial seeding density: 2,000 cells/well, n=6.

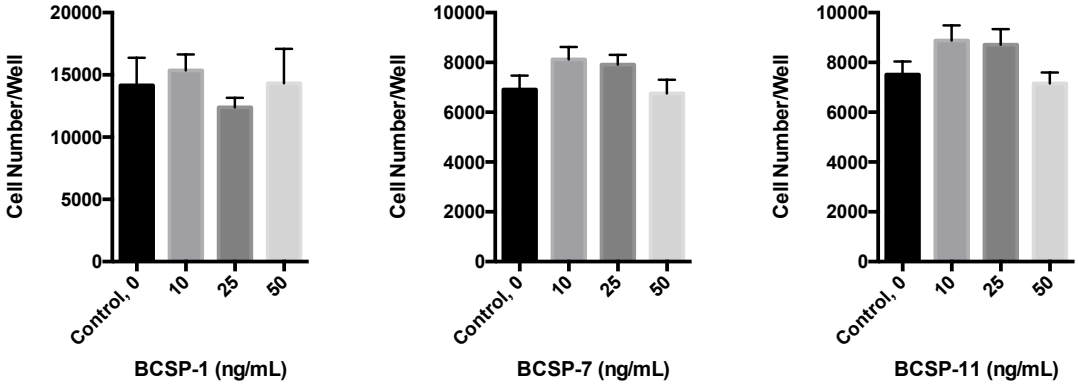

Figure 15. Proliferation assay result of human PDSCs. Initial seeding density of BCSP1 assay: 3,000 cells/well, initial seeding density of BCSP7 and BCSP11 assays: 2,000 cells/well, the dsDNA quantification assay was conducted 5 days after the initial cell seeding. n=6

4.2 Evidence of Early Differentiation

BCSP1, BCSP7 and BCSP11 was administered individually to the cells at dosages of 10 ng/mL added every second day and 50 ng/mL added every second day. The ALP expression level of MC3T3-E1 preosteoblasts [Figure 16] and hBM-MSCs [Figure 17] were assessed at days 7 and day 14, respectively, and the results are presented in nmol pNP/mg protein/min and fold-increase over control [Table 2].

In the assays with MC3T3-E1 preosteoblasts, the ALP expression was significantly enhanced to approximately two fold greater than control when treated for seven days with BCSP1 at 10 ng/mL (8.46 ± 1.56 nmol pNP/mg/min), BCSP7 at 50 ng/mL (9.16 ± 2.55 nmol pNP/mg/min) and BCSP11 at 10 ng/mL (9.31 ± 1.84 nmol pNP/mg/min). The

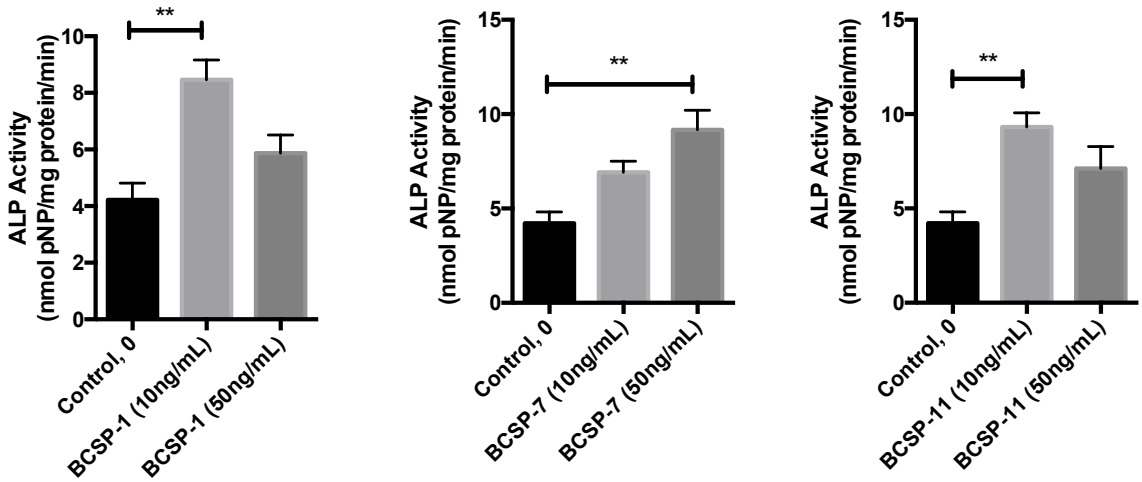

Figure 16. ALP expression assay result of MC3T3-E1 Preosteoblast. ALP expression assay was carried out at day 7 and the ALP activity is expressed in nmol pNP generated/mg protein/min, n=6.

ALP expression level in MC3T3-E1 preosteoblasts that were treated with the rest of the conditions also showed an increase; however, it was not significant.

In the experiments with hBM-MSCs, only BCSP1 and BCSP7 showed significant increases in ALP expression level. The ALP expression level of the treated hBM-MSCs increased two fold over that of the untreated hBM-MSCs after treatment with BCSP1 at both 10 ng/mL (26.96 ± 5.44 nmol pNP/mg/min) and 50 ng/mL (23.36 ± 2.31 nmol pNP/mg/min) or BCSP7 at 10 ng/mL (28.69 ± 3.25 nmol pNP/mg/min) over a period of 14 days. The cells treated with BCSP11 at 10 ng/mL and 50 ng/mL added every second day over a period of 14 days showed no significant increase in ALP expression level.

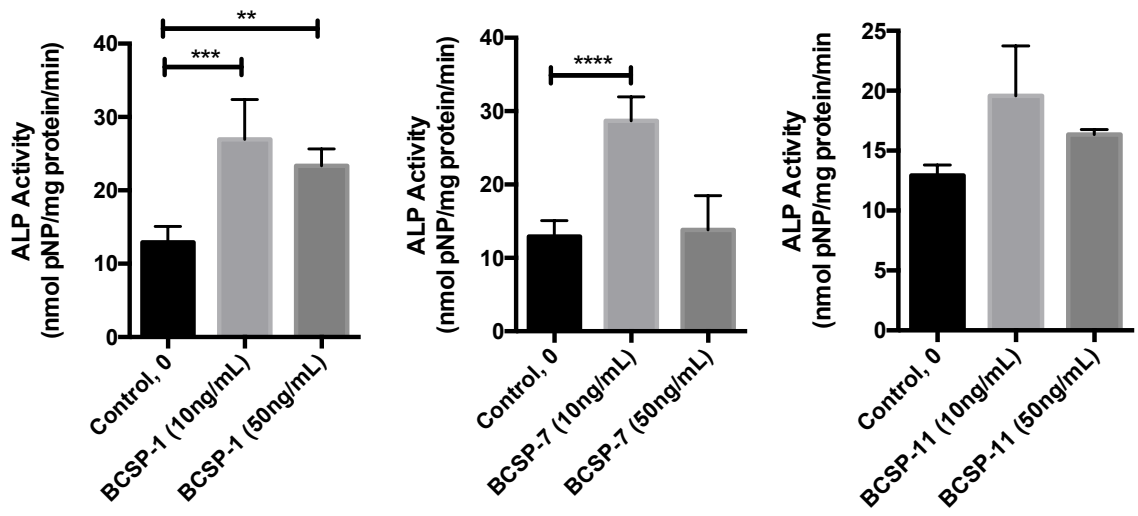

Figure 17. ALP expression assay result of human BM-MSCs. ALP expression assay was carried out at day 14 and the ALP activity is expressed in nmol pNP generated/mg protein/ min, n=6.

Table 2. Fold-increase of ALP expression level over control. ALP expression level of the BCSP-treated groups were normalized to the ALP expression level of the control groups (cultured in complete medium)

	BCSP-1 (10ng/mL)	BCSP-1 (50ng/mL)	BCSP-7 (10ng/mL)	BCSP-7 (50ng/mL)	BCSP-11 (10ng/mL)	BCSP-11 (50ng/mL)
MC3T3-E1	**2.01**	1.39	1.64	**2.17**	**2.21**	1.69
BM-MSCs	**2.09**	**1.81**	**2.22**	1.07	1.51	1.26

4.3 Mineralization

Each of BCSP1, BCSP7 and BCSP11 was administered at the dosage of 10 ng/mL or 50 ng/mL added every second day to MC3T3-E1 preosteoblasts over a period of 14 days and to hBM-MSCs over 21 days, followed by Alizarin Red S staining. Images of the positive control groups and pictures of the experimental group plates were taken and stains were quantified with dye extraction and absorbance measurement.

Mineral deposition was observed in the positive control groups of MC3T3-E1 preosteoblasts [Figure 18] and in the human BM-MSCs [Figure 19]. However, no mineral deposition were observed in the BCSP treatment groups. BCSP-treated groups of MC3T3-E1 preosteoblasts [Figure 20] and BM-MSCs [Figure 21] all stained negative. When quantified, no significant difference was found between the absorbance readings of BCSP treated groups and that of the control, either with MC3T3-E1 preosteoblast cells or human BM-MSCs [Figure 22].

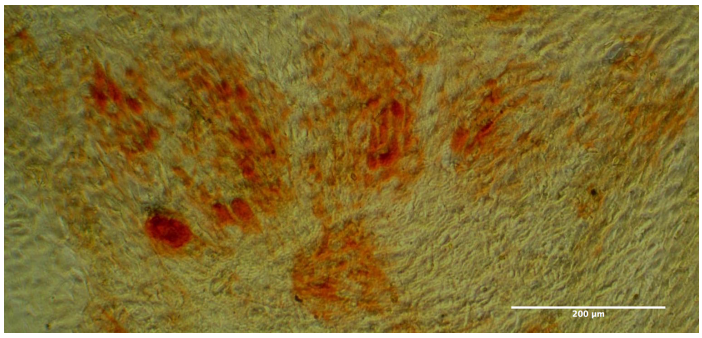

Figure 18. Alizarin Red S staining on the positive control of MC3T3-E1 Preosteoblast. Cells were seeded in the same seeding density (150,000 cells/well) and cultured in the osteogenic differentiation medium for the same period of time (14 days) as the BCSP-treated groups. Red staining is the dyed mineral deposition, which confirms the osteogenic capacity of the cells used in the experiment.

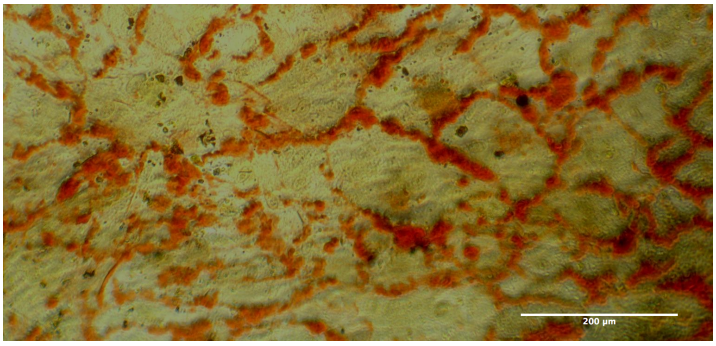

Figure 19. Alizarin Red S staining on the positive control of human BM-MSCs. Cells were seeded in the same seeding density (100,000 cells/well) and cultured in the osteogenic differentiation medium for the same period of time (21 days) as the BCSP-treated groups. Red staining is the dyed mineral deposition, which confirms the osteogenic capacity of the cells used in the experiment.

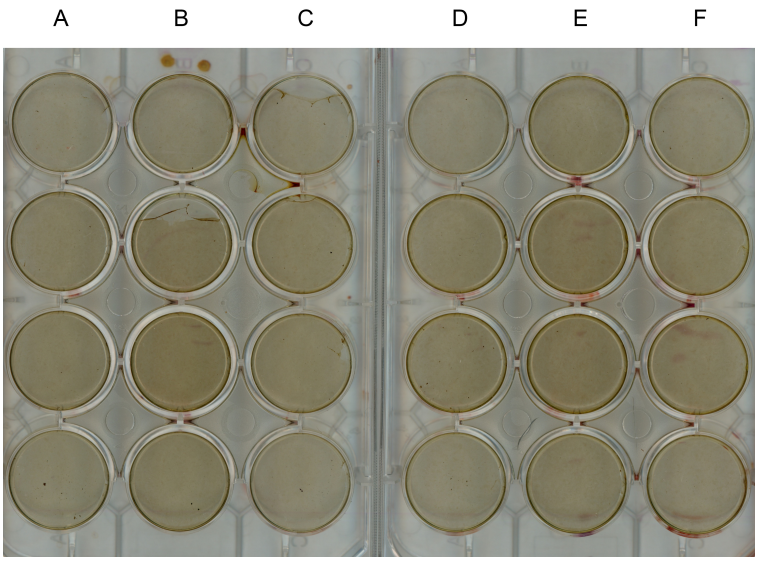

Figure 20. Alizarin Red S staining of BCSP treatment groups of MC3T3-E1 preosteoblast. Alizarin Red S staining was conducted after 14 days of BCSP treatment in the conditions listed and no mineral deposition was observed in any of the BCSP-treated groups. Treatment conditions in A-F: BCSP1 at 10 ng/mL, BCSP1 at 50 ng/mL, BCSP7 at 10 ng/mL, BCSP7 at 50 ng/mL, BCSP11 at 10 ng/mL, BCSP11 at 50 ng/mL

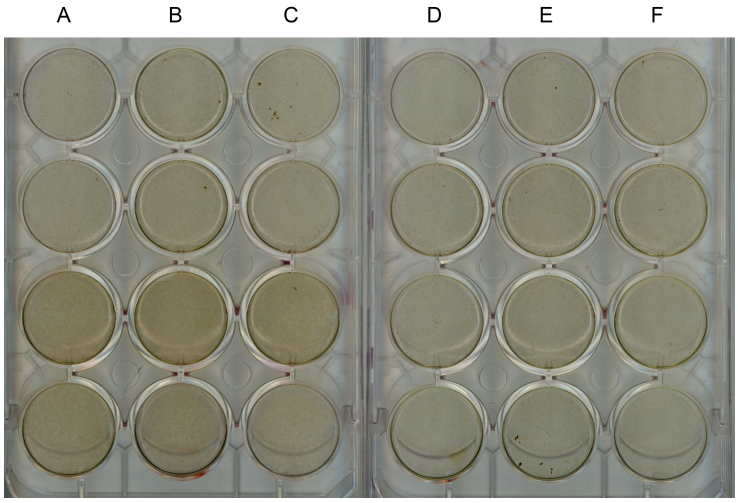

Figure 21. Alizarin Red S staining of BCSP treatment groups of hBM-MSCs. Alizarin Red S staining was conducted after 21 days of BCSP treatment in the conditions listed and no mineral deposition was observed in any of the BCSP-treated groups. Treatment conditions in A-F: BCSP1 at 10 ng/mL, BCSP1 at 50 ng/mL, BCSP7 at 10 ng/mL, BCSP7 at 50 ng/mL, BCSP11 at 10 ng/mL, BCSP11 at 50 ng/mL

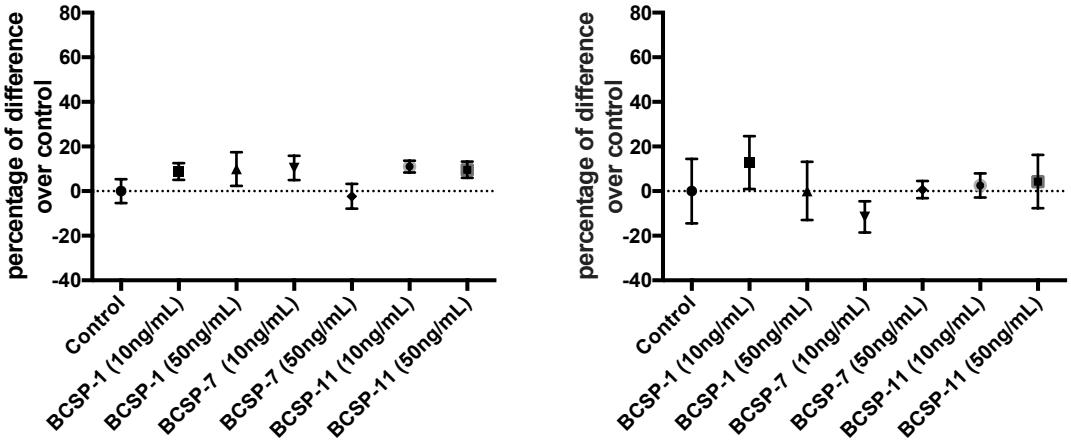

Figure 22. Alizarin Red S staining quantification of MC3T3-E1 preosteoblasts (left) and hBM-MSCs (right). Presented as percentage of difference of the absorbance of the BCSP treatment groups over that of control group. n=4

4.4 PDSC Characterization and Migration

The osteogenic differentiation potential of rPDSCs and hPDSCs were confirmed. Both rPDSCs [Figure 23] and hPDSCs [Figure 24] cultured in osteogenic medium stained positive for Von Kossa staining, indicated by the black nodules in the figures.

A migration assay was carried out 24 h after cell seeding, and cells that migrated through the membrane were counted to obtain the migration percentage. No significant difference of migration percentage was observed between any of the BCSP groups and the control groups. The migration of MC3T3-E1 preosteoblasts [Figure 25] and human PDSCs [Figure 26] did not significantly increase or decrease in the presence of BCSP1, BCSP7 or

BCSP11 at concentrations of 10, 25 and 50 ng/mL. Furthermore, no significant difference was observed in the migration of rPDSCs in the presence of BCSP1 compared to the control [Figure 27].

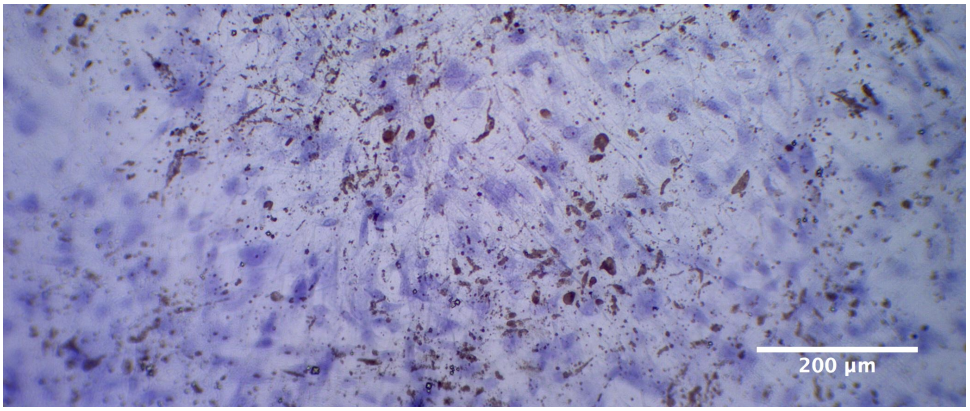

Figure 23. Von Kossa staining on the positive control of rabbit PDSCs. Black staining is the dyed mineral deposition.

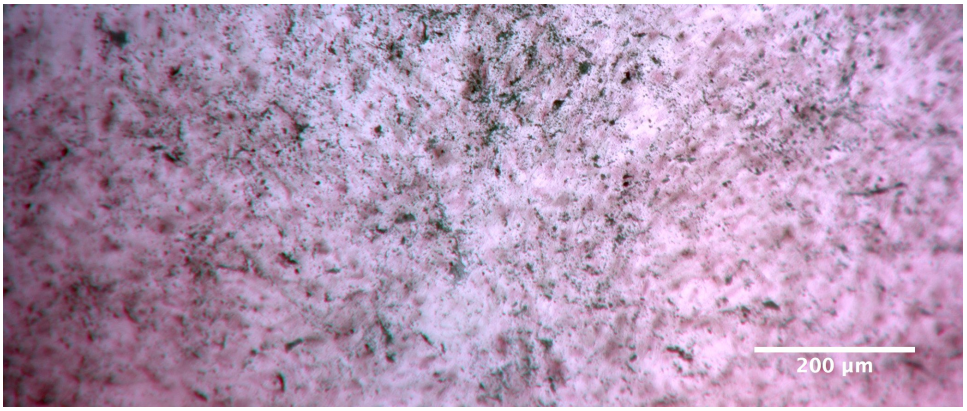

Figure 24. Von Kossa staining on the positive control of human PDSCs. Black staining is the dyed mineral deposition.

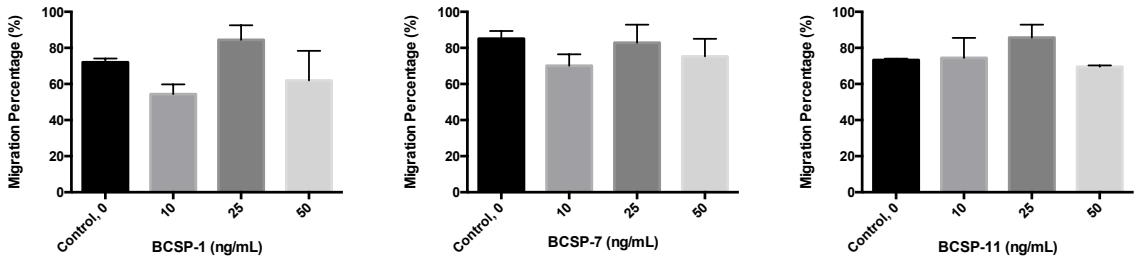

Figure 25. Migration assay result of MC3T3-E1 preosteoblasts. Migration assay was conducted 24 hours after cell seeding and the seeding density in the assay was 15,000 cells/insert, n=4.

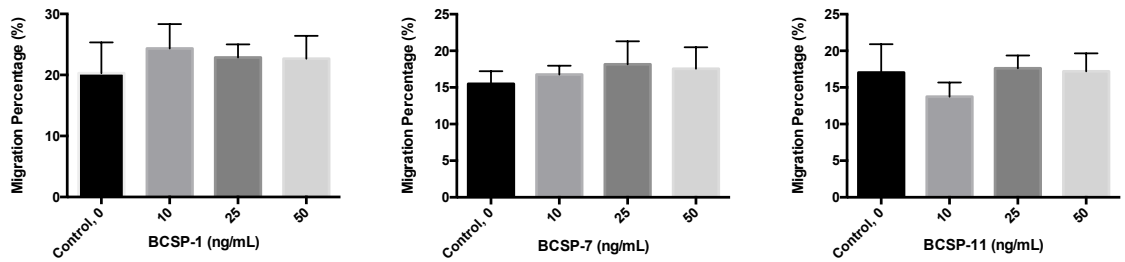

Figure 26. Migration assay result of hPDSCs. Migration assay was conducted 24 hours after the cells seeding. Seeding density in the assay is 30,000 cells/insert, n=4.

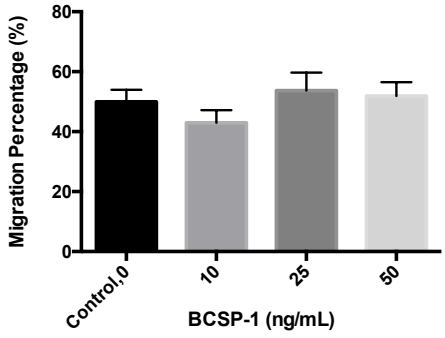

Figure 27. Migration assay result of rabbit PDSCs. Migration assay was conducted 24 hours after initial seeding and the seeding density was 9,000 cells/insert, n=6.

4.5 Results Summary

Results of the assays above are summarized in Table 3 below. Non-enhancing effects of the BCSPs examined are marked as "-" while positive effects of the BCSPs are indicated with BCSP type and effective concentrations.

Table 3. Screening Chart of BCSP Performance. Negative results are indicated as "—" and positive results are indicated by the BCSP type and the condition.

		BCSP1	BCSP7	BCSP11
Proliferation	MC3T3-E1	-	-	-
	BM-MSCs	-	-	-
	Human PDSCs	-	-	-
ALP Expression	MC3T3-E1	**BCSP1, 10ng/mL**	**BCSP7, 50ng/mL**	**BCSP11, 10ng/mL**
	BM-MSCs	**BCSP1, 10 and 50 ng/mL**	**BCSP7, 10ng/mL**	-
Mineral Formation	MC3T3-E1	-	-	-
	BM-MSCs	-	-	-
Cell migration	MC3T3-E1	-	-	-
	Human PDSCs	-	-	-
	Rabbit PDSCs	-		

Chapter 5: Discussion

5.1 Proliferation

Previous studies (90) indicated that BCSP1 had a dosage-dependent stimulating effect on the proliferation of bovine chondrocytes and human chondrocytes. However, the proliferation of MC3T3-E1 preosteoblasts, hBM-MSCs and hPDSCs were not enhanced by the treatment with various concentrations of BCSP1, BCSP7 or BCSP11. This inconsistency could be due to the differences of species and cell types. In addition, human BM-MSCs are multipotent stem cells and hPDSCs and MC3T3-E1 cells are undifferentiated osteoblast precursors and committed osteoblast precursors, whereas human and bovine chondrocytes are well-differentiated cell types. The difference of differentiation stages could also contribute to the inconsistency between this present study and the studies carried out previously.

As described above in the literature review about bone fracture healing, two types of ossification, intramembranous ossification and endochondral ossification, occur during the fracture healing, among which the endochondral ossification requires the cartilage tissue as a precursor for the following ossification. The non-stimulating effect of BCSPs on the proliferation of osteoprogenitors along with the stimulating effect of BCSP1 on the proliferation of chondrocytes suggest that the enhanced bone growth in the previous *in vivo* study may be attributed to the improvement in the endochondral ossification stage due to the enhanced proliferation of chondrocytes.

Cells are thought to slow down their proliferating activity once they are committed towards a specific lineage (in this case, the osteogenic lineage) and start the differentiation process (116). The non-stimulating effect of the BCSPs on proliferation that was observed may therefore be due to the cells becoming committed to the osteogenic phenotype.

5.2 Early differentiation and mineralization

ALP is commonly used as an early osteogenic marker of both MC3T3-E1 preosteoblasts and hBM-MSCs. Day 7 and day 14 are common time points to assess ALP expression level for both MC3T3-E1 preosteoblasts and BM-MSCs (117-119). Type I collagen matrix is laid down as the ALP expression level reaches its peak and declines afterwards. The matrix is then mineralized, which is a hallmark of the late stage of osteogenic differentiation. Mineralization reflects advanced osteogenic differentiation and the osteogenic outcome over a relatively long period of time both *in vivo* and *in vitro*. As described above, BCSP1 showed a stimulating effect on ALP expression in rat bone marrow-derived osteoprogenitors and rat calvaria-derived osteoprogenitors. BCSP1 and BCSP7 also significantly enhanced bone mineral formation and bone mineral density *in vivo* in a rabbit fracture healing model (90).

In the present work, BCSP1 and BCSP7 showed a stimulating effect on ALP expression level of both MC3T3-E1 preosteoblasts and human BM-MSCs, similar to the effects observed in previous studies, even though this present study was carried out with different cell sources. However, in the present study, no mineral deposition was observed on BCSP-treated cell culture, indicating that mineralization was not induced by BCSP1, BCSP7

or BCSP11 alone. Compared to the expression of a single marker such as ALP, mineralization is orchestrated by various factors and signal pathways, especially *in vivo.* Many factors, such as Runx2, Osterix, ALP, osteopontin and osteocalcin, play critical roles in the differentiation process of MSCs or pre-osteoblasts to the mature osteoblasts, and they are also critical in *in vitro* bone formation process from the newly seeded cell population to the mineralized cell culture (74, 120-122). Intracellular ALP is the early marker indicating the osteogenic differentiation commitment of the MSCs and the continued osteogenic differentiation from pre-osteoblast to mature osteoblasts. However, mineralization is the ultimate outcome of *in vitro* osteogenic differentiation which requires, at a molecular level, the expressions of critical factors as described above and, at a cellular level, the secretion of osteoid (mostly collagen I, unmineralized matrix) and its mineralization. Elevation of the early expression of ALP can be used to predict the long-term mineral deposition outcome but the elevated ALP expression level cannot guarantee a successful *in vitro* mineralization outcome. Evidence reported in the previous study indicated a 5-fold increase of ALP expression level *in vitro* that still failed to lead to *in vivo* bone formation (104), which supports the findings herein. The expression level of multiple markers, therefore, needs to be tested to acquire a better understanding of the potential differentiation stimulating effect of BCSPs.

5.3 Migration

Migration assays were conducted with cells in two differentiation phases: pre-osteoblasts and PDSCs. Pre-osteoblasts, or osteoblast precursors and multi-potential stem

cells make up the majority of the clinically beneficial cell population around the injury sites or post-surgery trauma sites that contribute to the healing process. Another possible mechanism, by which the *in vivo* bone formation observed in rabbits may have arisen, was through inducing the migration of osteoprogenitor cells to the site. However, the data in the present study indicates that neither MC3T3-E1 preosteoblasts nor human PDSCs increased cell migration under the influence of BCSP1, BCSP7 or BCSP11 at concentrations of 10, 25 or 50 ng/mL. This non-response at the concentrations listed suggests that BCSP1, BCSP7 and BCSP11 are not chemokines for MC3T3-E1 pre-osteoblasts and human PDSCs. In the migration assay with rabbit PDSCs and BCSP1, which mimics the cell type and BCSP type in the previous *in vivo* study, rabbit PDSCs also showed no increase in migration in the presence of BCSP1 at concentrations of 10, 25 and 50 ng/mL, suggesting that induction of PDSCs chemotaxis was not responsible for the enhanced bone formation shown in the previous *in vivo* study.

The cell population of rabbit PDSCs obtained in the present study were likely a mixture of various cell types including fibroblasts, fibroblast-like osteogenic cells, pre-osteoblasts, osteoblasts and mesenchymal stem cells. The migration assays conducted were done with un-sorted PDSCs and it is possible that BCSPs may function as a chemokine to specific cell types among the PDSCs cell population or to cells that are in a specific differentiation stage. However, the cells that are responsive to BCSPs might only make up a small portion of the entire population and this stimulating effect may be too small to be observed among other non-responding cells. Cell sorting and purification may therefore be required to further study the potential chemotactic function of BCSPs to PDSCs.

In this present study, BCSPs were suspended in the medium and the chemotactic migration of cells towards the presence of BCSPs were studied. The chemotactic migration was not observed since the number of the cells migrated was not increased with the presence of BCSPs, suggesting that the presence of the BCSPs in the medium have no stimulating effect on cell migration. However, when coated on the surface, BCSPs may be capable of stimulating the motility of the cells once they are attached to the coated surface. The global objective of this project is to design a autograft substitute incorporating a synthetic bone graft and the BCSPs. BCSPs may not be able to improve the recruitment of the osteogenic cell to the graft implant sites, however, BCSPs may have the potential to serve as osteoconductive factors to improve the cell motility and intragraft cell infiltration.

Chapter 6: Conclusions and Recommendations

6.1 Conclusions

The ALP expression level of MC3T3-E1 preosteoblasts was significantly increased in the presence of BCSP1, BCSP7 or BCSP11. The ALP expression level of hBM-MSCs was significantly increased in the presence of BCSP1 or BCSP7 but not in the presence of BCSP11. However, the elevation of the ALP expression level did not lead to the mineralization of the cell culture of both MC3T3-E1 preosteoblasts and hBM-MSCs in the presence of BCSP1, BCSP7 or BCSP11. These finding indicate that BCSPs have a stimulating effect on MC3T3-E1 and hBM-MSCs in the early osteogenic differentiation phase by enhancing the ALP expression but BCSP alone may not be able to initiate the *in vitro* mineralization. Furthermore, the proliferation of MC3T3-E1 preosteoblasts, hBM-MSCs and hPDSCs was not stimulated in the presence of the BCSP1, BCSP7 or BCSP11. The cell migration of MC3T3-E1 preosteoblasts and hPDSCs was not stimulated in the presence of BCSP1, BCSP7 or BCSP11, and the cell migration of rPDSCs was not stimulated in the presence of BCSP1 either. These findings suggest that the enhanced bone formation in the previous *in vivo* study was not attributed to the proliferation or the migration of osteoprogenitors.

6.2 Recommendations

Multiple markers are related to the osteogenic differentiation, and these markers regulate the outcomes of *in vitro* cell matrix mineralization and *in vivo* bone formation. Further assessment of the stimulating effect of osteogenic differentiation could include the expression of Runx2, osterix, osteocalcin (OC) and bone sialoprotein (BSP) as they are critical markers in both differentiation and mineral deposition.

In the mineralization assays, complete medium was used as control and experiments were conducted with complete medium with BCSPs but no mineralization was observed in BCSP treated groups. However, BCSPs might be able to promote the mineralization process once the mineralization is initiated. In the future studies, osteogenic medium could be used in both controls (osteogenic medium) and experiment conditions (osteogenic medium with BCSPs) so as to induce the mineralization before the assessment of BCSPs' stimulating effect. In the osteogenic differentiation assays, same design could also be used to assess whether the presence of BCSPs still promote the differentiation once the cells are committed to the osteogenic cell fate, with respect to enhancing the expression of osteogenic markers

Both *in vitro* mineralization and *in vivo* formation have two major steps: the formation of a un-mineralized collagenous matrix and the mineralization (*in vitro*) or ossification (*in vivo*) to form the bone tissue. The collagenous matrix is largely comprised of collagen Type I, therefore a staining specific to collagen type I could be used prior to the mineralization assay to assess the stimulating effect of BCSPs on un-mineralized matrix secretion.

In vitro mineralization is the hallmark of osteogenic differentiation and a useful biological parameter to measure the performance of a specific osteogenic cell type or the osteogenic enhancing activity of an agent. However, *in vivo* environment is more complex than the *in vitro* environment where cells are isolated from tissues and ECM. Enhanced *in vivo* bone growth is the ultimate goal of this project, therefore, an *in vivo* study with animal model of bone fracture is necessary to assess the overall performance of BCSPs.

References

1. Andersson GBJ. Epidemiological features of chronic low-back pain. The Lancet 1999;354(9178):581-585.

2. Deyo RA, Tsui-Wu YJ. Descriptive epidemiology of low-back pain and its related medical care in the united states. Spine (Phila Pa 1976) 1987;12(3):264-268.

3. Luo X, Pietrobon R, Sun SX, Liu GG, Hey L. Estimates and patterns of direct health care expenditures among individuals with back pain in the united states. Spine (Phila Pa 1976) 2004;29(1):79-86.

4. Taimela S, Kujala UM, Salminen JJ, Viljanen T. The prevalence of low back pain among children and adolescents. A nationwide, cohort-based questionnaire survey in finland. Spine (Phila Pa 1976) 1997;22(10):1132-1136.

5. Ekman M, Jonhagen S, Hunsche E, Jonsson L. Burden of illness of chronic low back pain in sweden: A cross-sectional, retrospective study in primary care setting. Spine (Phila Pa 1976) 2005;30(15):1777-1785.

6. Wenig CM, Schmidt CO, Kohlmann T, Schweikert B. Costs of back pain in germany. European journal of pain (London, England) 2009;13(3):280-286.

7. Deyo RAMDMPH, Weinstein JNDO. Low back pain. The New England Journal of Medicine 2001;344(5):363-370.

8. Samartzis D, Karppinen J, Chan D, Luk KD, Cheung KM. The association of lumbar intervertebral disc degeneration on magnetic resonance imaging with body mass

index in overweight and obese adults: A population-based study. Arthritis Rheum 2012;64(5):1488-1496.

9. Samartzis D, Karppinen J, Luk K, Cheung K. Baseline mri characteristics in asymptomatic subjects as predictors for future first-time lbp episode.

10. Miller JAA, Schmatz C, Schultz AB. Lumbar-disk degeneration - correlation with age, sex, and spine level in 600 autopsy specimens. Spine 1988;13(2):173-178.

11. Buckwalter JA. Spine update - aging and degeneration of the human intervertebral disc. Spine 1995;20(11):1307-1314.

12. Weinstein SL, Buckwalter JA. Turek's orthopaedics: Principles and their application: Lippincott Williams & Wilkins; 2005.

13. Eyre DR, Muir H. Quantitative analysis of types i and ii collagens in human intervertebral discs at various ages. Biochimica et Biophysica Acta (BBA) - Protein Structure 1977;492(1):29-42.

14. Choi Y-S. Pathophysiology of degenerative disc disease. Asian spine journal 2009;3(1):39-44.

15. Ramani P. Textbook of surgical management of lumbar disc herniation: Jaypee Brothers,Medical Publishers Pvt. Limited; 2013.

16. Urban JP, McMullin JF. Swelling pressure of the lumbar intervertebral discs: Influence of age, spinal level, composition, and degeneration. Spine (Phila Pa 1976) 1988;13(2):179-187.

17. Kepler CK, Anderson DG, Tannoury C, Ponnappan RK. Intervertebral disk degeneration and emerging biologic treatments. The Journal of the American Academy of Orthopaedic Surgeons 2011;19(9):543-553.

18. Lyons G, Eisenstein SM, Sweet MB. Biochemical changes in intervertebral disc degeneration. Biochim Biophys Acta 1981;673(4):443-453.

19. Frobin W, Brinckmann P, Kramer M, Hartwig E. Height of lumbar discs measured from radiographs compared with degeneration and height classified from mr images. European Radiology 2001;11(2):263-269.

20. Adams MA, Dolan P, Hutton WC, Porter RW. Diurnal changes in spinal mechanics and their clinical-significance. Journal of Bone and Joint Surgery-British Volume 1990;72(2):266-270.

21. Urban JPG, Roberts S. Degeneration of the intervertebral disc. Arthritis Research & Therapy 2003;5(3):120-130.

22. Osti OL, Vernon-Roberts B, Fraser RD. 1990 volvo award in experimental studies. Anulus tears and intervertebral disc degeneration. An experimental study using an animal model. Spine (Phila Pa 1976) 1990;15(8):762-767.

23. Lotz JC, Colliou OK, Chin JR, Duncan NA, Liebenberg E. 1998 volvo award winner in biomechanical studies - compression-induced degeneration of the intervertebral disc: An in vivo mouse model and finite-element study. Spine 1998;23(23):2493-2506.

24. Maroudas A. Biophysical chemistry of cartilaginous tissues with special reference to solute and fluid transport. Biorheology 1975;12(3-4):233-248.

25. Lee J-W, Lee S, Lee SH, Yang HS, Im G, II, Kim C-S, Park J-H, Kim BS. Improved spinal fusion efficacy by long-term delivery of bone morphogenetic protein-2 in a rabbit model. Acta orthopaedica 2011;82(6):756-760.

26. Chong E, Pelletier MH, Mobbs RJ, Walsh WR. The design evolution of interbody cages in anterior cervical discectomy and fusion: A systematic review. BMC Musculoskeletal Disorders 2015;16:99.

27. Rajaee SS, Bae HW, Kanim LE, Delamarter RB. Spinal fusion in the united states: Analysis of trends from 1998 to 2008. Spine (Phila Pa 1976) 2012;37(1):67-76.

28. Weiss AJ, Elixhauser A, Andrews RM. Characteristics of operating room procedures in u.S. Hospitals, 2011: Statistical brief #170. Healthcare cost and utilization project (hcup) statistical briefs. Rockville (MD); 2006.

29. Weiss AJ, Elixhauser A. Trends in operating room procedures in u.S. Hospitals, 2001-2011: Statistical brief #171. Healthcare cost and utilization project (hcup) statistical briefs. Rockville (MD); 2006.

30. West JL, 3rd, Bradford DS, Ogilvie JW. Results of spinal arthrodesis with pedicle screw-plate fixation. The Journal of bone and joint surgery American volume 1991;73(8):1179-1184.

31. Bridwell KH, Sedgewick TA, Obrien MF, Lenke LG, Baldus C. The role of fusion and instrumentation in the treatment of degenerative spondylolisthesis with spinal stenosis. Journal of Spinal Disorders 1993;6(6):461-472.

32. McGuire RA, Amundson GM. The use of primary internal fixation in spondylolisthesis. Spine (Phila Pa 1976) 1993;18(12):1662-1672.

33. Zdeblick TA. A prospective, randomized study of lumbar fusion - preliminary-results. Spine 1993;18(8):983-991.

34. Hibbs RA. Xii. An operation for stiffening the knee-joint: With report of cases from the service of the new york orthopaedic hospital. Annals of surgery 1911;53(3): 404-407.

35. Silber JS, Anderson DG, Daffner SD, Brislin BT, Leland JM, Hilibrand AS, Vaccaro AR, Albert TJ. Donor site morbidity after anterior iliac crest bone harvest for single-level anterior cervical discectomy and fusion. Spine 2003;28(2):134-139.

36. Rubin R, Strayer DS, Rubin E, McDonald JM. Rubin's pathology: Clinicopathologic foundations of medicine: Lippincott Williams & Wilkins; 2008.

37. Revell PA. Pathology of bone: Springer London; 2012.

38. Enlow DH. Functions of the haversian system. American Journal of Anatomy 1962;110(3):269-305.

39. Bronner F, Worrell RV. Orthopaedics: Principles of basic and clinical science: Taylor & Francis; 1999.

40. McCarthy EF, Frassica FJ. Pathology of bone and joint disorders print and online bundle: Cambridge University Press; 2014.

41. Ellis RE. The distribution of active bone marrow in the adult. Physics in Medicine and Biology 1961;5(3):255.

42. Colnot C. Skeletal cell fate decisions within periosteum and bone marrow during bone regeneration. Journal of bone and mineral research : the official journal of the American Society for Bone and Mineral Research 2009;24(2):274-282.

43. Anselme K. Osteoblast adhesion on biomaterials. Biomaterials 2000;21(7): 667-681.

44. Clarke B. Normal bone anatomy and physiology. Clinical Journal of the American Society of Nephrology : CJASN 2008;3(Suppl 3):S131-139.

45. Ramalingam M, Wang X, Chen G, Ma P, Cui FZ. Biomimetics: Advancing nanobiomaterials and tissue engineering: Wiley; 2013.

46. Pajevic PD. Regulation of bone resorption and mineral homeostasis by osteocytes. IBMS BoneKEy 2009;6(2):63-70.

47. You L, Temiyasathit S, Lee P, Kim CH, Tummala P, Yao W, Kingery W, Malone AM, Kwon RY, Jacobs CR. Osteocytes as mechanosensors in the inhibition of bone resorption due to mechanical loading. Bone 2008;42(1):172-179.

48. O'Brien CA, Nakashima T, Takayanagi H. Osteocyte control of osteoclastogenesis. Bone 2013;54(2):258-263.

49. Takahashi N, Udagawa N, Suda T. Vitamin d endocrine system and osteoclasts. BoneKEy Rep 2014;3.

50. Khan KUhbgcbip-v. Physical activity and bone health: Human Kinetics; 2001.

51. Mundy GR. Bone remodelling and its disorders: Taylor & Francis; 1999.

52. Rousselle AV, Heymann D. Osteoclastic acidification pathways during bone resorption. Bone 2002;30(4):533-540.

53. Baron R, Neff L, Louvard D, Courtoy PJ. Cell-mediated extracellular acidification and bone resorption: Evidence for a low ph in resorbing lacunae and localization of a 100-kd lysosomal membrane protein at the osteoclast ruffled border. The Journal of cell biology 1985;101(6):2210-2222.

54. Zaidi M, Datta HK, Patchell A, Moonga B, MacIntyre I. 'Calcium-activated' intracellular calcium elevation: A novel mechanism of osteoclast regulation. Biochemical and Biophysical Research Communications 1989;163(3):1461-1465.

55. Lorget F, Kamel S, Mentaverri R, Wattel A, Naassila M, Maamer M, Brazier M. High extracellular calcium concentrations directly stimulate osteoclast apoptosis. Biochem Biophys Res Commun 2000;268(3):899-903.

56. Nielsen RH, Karsdal MA, Sørensen MG, Dziegiel MH, Henriksen K. Dissolution of the inorganic phase of bone leading to release of calcium regulates osteoclast survival. Biochemical and Biophysical Research Communications 2007;360(4):834-839.

57. Goldman L, Schafer AI. Goldman's cecil medicine: Elsevier Health Sciences; 2011.

58. Kapinas K, Delany AM. Microrna biogenesis and regulation of bone remodeling. Arthritis Research & Therapy 2011;13(3):220-220.

59. Parfitt AM. The cellular basis of bone remodeling: The quantum concept reexamined in light of recent advances in the cell biology of bone. Calcif Tissue Int 1984;36 Suppl 1:S37-45.

60. Miller SC, de Saint-Georges L, Bowman BM, Jee WS. Bone lining cells: Structure and function. Scanning microscopy 1989;3(3):953-960; discussion 960-951.

61. Bilezikian JP, Raisz LG, Rodan GA. Principles of bone biology, two-volume set: Elsevier Science; 2002.

62. Bruzzaniti A, Baron R. Molecular regulation of osteoclast activity. Reviews in endocrine & metabolic disorders 2006;7(1-2):123-139.

63. Murray DW, Rushton N. Macrophages stimulate bone resorption when they phagocytose particles. The Journal of bone and joint surgery British volume 1990;72(6): 988-992.

64. Lassus J, Salo J, Jiranek WA, Santavirta S, Nevalainen J, Matucci-Cerinic M, Horak P, Konttinen Y. Macrophage activation results in bone resorption. Clin Orthop Relat Res 1998(352):7-15.

65. Hauschka PV, Chen TL, Mavrakos AE. Polypeptide growth factors in bone matrix. Ciba Foundation symposium 1988;136:207-225.

66. Matsuo K, Irie N. Osteoclast-osteoblast communication. Archives of biochemistry and biophysics 2008;473(2):201-209.

67. Kim S, Kang Y, Krueger CA, Sen M, Holcomb JB, Chen D, Wenke JC, Yang Y. Sequential delivery of bmp-2 and igf-1 using a chitosan gel with gelatin microspheres enhances early osteoblastic differentiation. Acta Biomater 2012;8(5):1768-1777.

68. Fakhry M, Hamade E, Badran B, Buchet R, Magne D. Molecular mechanisms of mesenchymal stem cell differentiation towards osteoblasts. World Journal of Stem Cells 2013;5(4):136-148.

69. Dominici M, Le Blanc K, Mueller I, Slaper-Cortenbach I, Marini F, Krause D, Deans R, Keating A, Prockop D, Horwitz E. Minimal criteria for defining multipotent mesenchymal stromal cells. The international society for cellular therapy position statement. Cytotherapy 2006;8(4):315-317.

70. Takarada T, Hinoi E, Nakazato R, Ochi H, Xu C, Tsuchikane A, Takeda S, Karsenty G, Abe T, Kiyonari H, Yoneda Y. An analysis of skeletal development in osteoblast-specific and chondrocyte-specific runt-related transcription factor-2 (runx2) knockout mice. Journal of bone and mineral research : the official journal of the American Society for Bone and Mineral Research 2013;28(10):2064-2069.

71. Komori T. Regulation of osteoblast differentiation by runx2. In: Choi Y, editor. Osteoimmunology: Interactions of the immune and skeletal systems ii. Boston, MA: Springer US; 2010. p. 43-49.

72. Nakashima K, Zhou X, Kunkel G, Zhang Z, Deng JM, Behringer RR, de Crombrugghe B. The novel zinc finger-containing transcription factor osterix is required for osteoblast differentiation and bone formation. Cell 2002;108(1):17-29.

73. Golub EE, Boesze-Battaglia K. The role of alkaline phosphatase in mineralization. Current Opinion in Orthopaedics 2007;18(5):444-448.

74. Collin P, Nefussi JR, Wetterwald A, Nicolas V, Boy-Lefevre M-L, Fleisch H, Forest N. Expression of collagen, osteocalcin, and bone alkaline phosphatase in a mineralizing rat osteoblastic cell culture. Calcified Tissue International;50(2):175-183.

75. Zhang X, Aubin JE, Inman RD. Molecular and cellular biology of new bone formation: Insights into the ankylosis of ankylosing spondylitis. Current opinion in rheumatology 2003;15(4):387-393.

76. Aubin JE. Regulation of osteoblast formation and function. Reviews in endocrine & metabolic disorders 2001;2(1):81-94.

77. Tye CE, Hunter GK, Goldberg HA. Identification of the type i collagen-binding domain of bone sialoprotein and characterization of the mechanism of interaction. The Journal of biological chemistry 2005;280(14):13487-13492.

78. Weinreb M, Shinar D, Rodan GA. Different pattern of alkaline phosphatase, osteopontin, and osteocalcin expression in developing rat bone visualized by in situ hybridization. Journal of bone and mineral research : the official journal of the American Society for Bone and Mineral Research 1990;5(8):831-842.

79. Chenu C, Colucci S, Grano M, Zigrino P, Barattolo R, Zambonin G, Baldini N, Vergnaud P, Delmas PD, Zallone AZ. Osteocalcin induces chemotaxis, secretion of matrix proteins, and calcium-mediated intracellular signaling in human osteoclast-like cells. The Journal of cell biology 1994;127(4):1149-1158.

80. Cruess RL, Dumont J. Fracture healing. Canadian journal of surgery Journal canadien de chirurgie 1975;18(5):403-413.

81. Casanova M, Schindeler A, Little D, Muller R, Schneider P. Quantitative phenotyping of bone fracture repair: A review. BoneKEy Rep 2014;3.

82. Glowacki J. Angiogenesis in fracture repair. Clin Orthop Relat Res 1998(355 Suppl):S82-89.

83. Phillips FM, Lieberman IH, Polly DW. Minimally invasive spine surgery: Springer; 2014.

84. Echeverri LF, Herrero MA, Lopez JM, Oleaga G. Early stages of bone fracture healing: Formation of a fibrin-collagen scaffold in the fracture hematoma. Bulletin of mathematical biology 2015;77(1):156-183.

85. Einhorn TA. The cell and molecular biology of fracture healing. Clin Orthop Relat Res 1998(355 Suppl):S7-21.

86. Bolander ME. Regulation of fracture repair by growth factors. Proceedings of the Society for Experimental Biology and Medicine Society for Experimental Biology and Medicine (New York, NY) 1992;200(2):165-170.

87. Boden SD, Schimandle JH, Hutton WC, Chen MI. The use of an osteoinductive growth factor for lumbar spinal fusion .1. Biology of spinal fusion. Spine 1995;20(24):2626-2632.

88. Miyazaki M, Tsumura H, Wang JC, Alanay A. An update on bone substitutes for spinal fusion. Eur Spine J 2009;18(6):783-799.

89. Rosenblum B. Current update on orthobiologics in foot and ankle surgery, an issue of clinics in podiatric medicine and surgery: Elsevier Health Sciences; 2014.

90. Sindrey D, Pugh S, Smith T. Connective tissue stimulating peptides. Google Patents; 2005.

91. Sudo H, Kodama HA, Amagai Y, Yamamoto S, Kasai S. In vitro differentiation and calcification in a new clonal osteogenic cell line derived from newborn mouse calvaria. The Journal of cell biology 1983;96(1):191-198.

92. Wang D, Christensen K, Chawla K, Xiao G, Krebsbach PH, Franceschi RT. Isolation and characterization of mc3t3-e1 preosteoblast subclones with distinct in vitro and in vivo differentiation/mineralization potential. Journal of bone and mineral research : the official journal of the American Society for Bone and Mineral Research 1999;14(6):893-903.

93. Sowa H, Kaji H, Canaff L, Hendy GN, Tsukamoto T, Yamaguchi T, Miyazono K, Sugimoto T, Chihara K. Inactivation of menin, the product of the multiple endocrine neoplasia type 1 gene, inhibits the commitment of multipotential mesenchymal stem cells into the osteoblast lineage. The Journal of biological chemistry 2003;278(23): 21058-21069.

94. Kim JL, Park SH, Jeong D, Nam JS, Kang YH. Osteogenic activity of silymarin through enhancement of alkaline phosphatase and osteocalcin in osteoblasts and tibia-fractured mice. Experimental biology and medicine (Maywood, NJ) 2012;237(4): 417-428.

95. Nishide Y, Tousen Y, Tadaishi M, Inada M, Miyaura C, Kruger MC, Ishimi Y. Combined effects of soy isoflavones and beta-carotene on osteoblast differentiation. International journal of environmental research and public health 2015;12(11):13750-13761.

96. Niska K, Pyszka K, Tukaj C, Wozniak M, Radomski MW, Inkielewicz-Stepniak I. Titanium dioxide nanoparticles enhance production of superoxide anion and alter the antioxidant system in human osteoblast cells. International journal of nanomedicine 2015;10:1095-1107.

97. Baksh D, Yao R, Tuan RS. Comparison of proliferative and multilineage differentiation potential of human mesenchymal stem cells derived from umbilical cord and bone marrow. STEM CELLS 2007;25(6):1384-1392.

98. Li ZY, Chen L, Liu L, Lin YF, Li SW, Tian WD. Odontogenic potential of bone marrow mesenchymal stem cells. Journal of oral and maxillofacial surgery : official journal of the American Association of Oral and Maxillofacial Surgeons 2007;65(3): 494-500.

99. Batsali A, Kouvidi E, Damianaki A, Stratigi A, Kastrinaki M-C, Papadaki HA. Comparative analysis of bone marrow and wharton's jelly mesenchymal stem/stromal cells. Blood 2013;122(21):1212-1212.

100. Fayaz HC, Giannoudis PV, Vrahas MS, Smith RM, Moran C, Pape HC, Krettek C, Jupiter JB. The role of stem cells in fracture healing and nonunion. International Orthopaedics 2011;35(11):1587-1597.

101. Gómez-Barrena E, Rosset P, Müller I, Giordano R, Bunu C, Layrolle P, Konttinen YT, Luyten FP. Bone regeneration: Stem cell therapies and clinical studies in

orthopaedics and traumatology. Journal of Cellular and Molecular Medicine 2011;15(6): 1266-1286.

102. Quarto R, Mastrogiacomo M, Cancedda R, Kutepov SM, Mukhachev V, Lavroukov A, Kon E, Marcacci M. Repair of large bone defects with the use of autologous bone marrow stromal cells. N Engl J Med 2001;344(5):385-386.

103. Kim S-J, Shin Y-W, Yang K-H, Kim S-B, Yoo M-J, Han S-K, Im S-A, Won Y-D, Sung Y-B, Jeon T-S, Chang C-H, Jang J-D, Lee S-B, Kim H-C, Lee S-Y. A multi-center, randomized, clinical study to compare the effect and safety of autologous cultured osteoblast(ossron™) injection to treat fractures. BMC Musculoskeletal Disorders 2009;10:20-20.

104. Prins H-J, Braat AK, Gawlitta D, Dhert WJA, Egan DA, Tijssen-Slump E, Yuan H, Coffer PJ, Rozemuller H, Martens AC. In vitro induction of alkaline phosphatase levels predicts in vivo bone forming capacity of human bone marrow stromal cells. Stem Cell Research 2014;12(2):428-440.

105. Dwek JR. The periosteum: What is it, where is it, and what mimics it in its absence? Skeletal Radiology 2010;39(4):319-323.

106. Squier CA, Ghoneim S, Kremenak CR. Ultrastructure of the periosteum from membrane bone. J Anat 1990;171:233-239.

107. Diaz-Flores L, Gutierrez R, Lopez-Alonso A, Gonzalez R, Varela H. Pericytes as a supplementary source of osteoblasts in periosteal osteogenesis. Clin Orthop Relat Res 1992(275):280-286.

108. Chen FG, Zhang WJ, Bi D, Liu W, Wei X, Chen FF, Zhu L, Cui L, Cao Y. Clonal analysis of nestin(-) vimentin(+) multipotent fibroblasts isolated from human dermis. Journal of cell science 2007;120(Pt 16):2875-2883.

109. Youn I, Suh JK, Nauman EA, Jones DG. Differential phenotypic characteristics of heterogeneous cell population in the rabbit periosteum. Acta orthopaedica 2005;76(3):442-450.

110. Agata H, Asahina I, Yamazaki Y, Uchida M, Shinohara Y, Honda MJ, Kagami H, Ueda M. Effective bone engineering with periosteum-derived cells. Journal of dental research 2007;86(1):79-83.

111. Hayashi O, Katsube Y, Hirose M, Ohgushi H, Ito H. Comparison of osteogenic ability of rat mesenchymal stem cells from bone marrow, periosteum, and adipose tissue. Calcif Tissue Int 2008;82(3):238-247.

112. Ribeiro FV, Suaid FF, Ruiz KG, Salmon CR, Paparotto T, Nociti FH, Jr., Sallum EA, Casati MZ. Periosteum-derived cells as an alternative to bone marrow cells for bone tissue engineering around dental implants. A histomorphometric study in beagle dogs. Journal of periodontology 2010;81(6):907-916.

113. Stevens MM, Marini RP, Schaefer D, Aronson J, Langer R, Shastri VP. In vivo engineering of organs: The bone bioreactor. Proceedings of the National Academy of Sciences of the United States of America 2005;102(32):11450-11455.

114. Alberts B, Johnson A, Lewis J, Raff M, Roberts K, Walter P. Molecular biology of the cell, fourth edition: Garland Science; 2002.

115. Hulkower KI, Herber RL. Cell migration and invasion assays as tools for drug discovery. Pharmaceutics 2011;3(1):107-124.

116. Lanza RP. Handbook of stem cells: Elsevier Academic; 2004.

117. Takeuchi Y, Nakayama K, Matsumoto T. Differentiation and cell surface expression of transforming growth factor-beta receptors are regulated by interaction with matrix collagen in murine osteoblastic cells. The Journal of biological chemistry 1996;271(7):3938-3944.

118. Yazid MD, Ariffin SHZ, Senafi S, Razak MA, Wahab RMA. Determination of the differentiation capacities of murines' primary mononucleated cells and mc3t3-e1 cells. Cancer Cell International 2010;10:42-42.

119. Alves EG, Serakides R, Boeloni JN, Rosado IR, Ocarino NM, Oliveira HP, Góes AM, Rezende CM. Comparison of the osteogenic potential of mesenchymal stem cells from the bone marrow and adipose tissue of young dogs. BMC Veterinary Research 2014;10(1):1-9.

120. Gordon JAR, Tye CE, Sampaio AV, Underhill TM, Hunter GK, Goldberg HA. Bone sialoprotein expression enhances osteoblast differentiation and matrix mineralization in vitro. Bone;41(3):462-473.

121. Byers BA, Garcia AJ. Exogenous runx2 expression enhances in vitro osteoblastic differentiation and mineralization in primary bone marrow stromal cells. Tissue Eng 2004;10(11-12):1623-1632.

122. Holm E, Gleberzon JS, Liao Y, Sorensen ES, Beier F, Hunter GK, Goldberg HA. Osteopontin mediates mineralization and not osteogenic cell development in vitro. The Biochemical journal 2014;464(3):355-364.